JOURNAL OF GEOPHYSICAL RESEARCH, VOL. 96, NO. C8, PAGES 14,707–14,730, AUGUST 15, 1991

# The Structure of the Transition Zone Between Coastal Waters and the Open Ocean off Northern California, Winter and Spring 1987

P. MICHAEL KOSRO,[1] ADRIANA HUYER,[1] STEVEN R. RAMP,[2] ROBERT L. SMITH,[1]
FRANCISCO P. CHAVEZ,[3] TIMOTHY J. COWLES,[1] MARK R. ABBOTT,[1] P. TED STRUB,[1]
RICHARD T. BARBER,[4] PAUL JESSEN,[2] AND LAWRENCE F. SMALL[1]

Physical and biological fields in the coastal transition zone off northern California were measured during February, March, May and June 1987 in an extended alongshore region between 60 km and 150 km offshore. The spring transition, as seen in coastal sea level and winds, occurred in mid-March. Surface variability during the two spring cruises was stronger and of larger scale than that seen during the two winter cruises. An equatorward-tending current, flowing along the boundary between low steric sea level inshore and high steric sea level offshore, dominated both the directly-measured (acoustic Doppler current profiler) and geostrophic current fields during spring. Current jets of comparable strength directed both offshore and onshore were seen off Cape Mendocino and Point Arena; these evolved significantly in the 3 weeks between cruises. Inshore of the current, properties associated with upwelled water were found near the surface, including low temperature and high salinity, nutrients and chlorophyll; offshore of the current, waters were warmer, less saline, lower in nutrients and more oligotrophic. Geostrophic and directly measured volume transports in the current were about 2–3 Sv. Isopycnals inshore of the spring upwelling front were displaced vertically by $O$(40–80 m) from their depths during the winter survey; these displacements extended deep into the water column and were largely independent of depth between 100 and 400 m. Surface mixed layers tended to be deep in winter and shallower inshore of the upwelling front in spring. A connection between the equatorward-tending frontal jet off northern California and the more well-studied California Current further south is suggested by the similarity of their transports and of their dynamic height values.

## 1. INTRODUCTION

Over the past decade, in situ and satellite observations of the waters off northern California have revealed the inhomogeneous nature of the transition zone between coastal and offshore waters during the spring-summer upwelling season. During the upwelling season, coastal waters lying over the continental shelf and upper slope of northern California are cold, high in salinity [*Robinson*, 1976; *Huyer and Kosro*, 1987], and generally high in nutrients [*Traganza et al.*, 1980]; coastal currents respond rapidly to the local wind stress which varies on time scales of days [*Winant et al.*, 1987]. Offshore, surface waters are warm and relatively fresh [*Robinson*, 1976; *Lynn et al.*, 1982]; they flow generally southward in an eastern boundary current (most often sampled south of 38°N) which contains mesoscale eddies [*Wooster and Reid*, 1963; *Wyllie*, 1966].

Satellite images of the transition zone have shown long tongues or filaments of cold, high-chlorophyll water extending from the coastal zone to more than 200 km from shore [*Bernstein et al.*, 1977; *Abbott and Zion*, 1985]. At least some of these cold tongues and filaments are associated with strong (>0.5 m/s), narrow (~30 km), seaward currents [*Davis*, 1985; *Kosro*, 1985; *Rienecker et al.*, 1985; *Flament et al.*, 1985; *Kosro and Huyer*, 1986].

Surface drifters deployed over the shelf near Point Arena [*Davis*, 1985] suggested that freshly upwelled waters may "squirt" directly offshore, after undergoing little or no alongshore displacement. Other observations, including a May 1977 survey of northern California slope waters [*Freitag and Halpern*, 1981] and a July 1982 survey of waters offshore of Point Arena [*Kosro and Huyer*, 1986], suggested that the seaward jet off Point Arena is a continuation of a strong alongshore "coastal jet" that flows generally southward along the upwelling front between warmer offshore waters and cold, freshly-upwelled coastal waters. This view is supported by the track of a drifter which moved rapidly southward at about 125°W between 45°N and 35°N in August and September 1984 [*Thomson and Papadakis*, 1987] and it is implicit in the *Ikeda and Emery* [1984] model of California Current meanders. Still other observations [*Mooers and Robinson*, 1984; *Rienecker and Mooers*, 1989] suggested that pairs of oppositely rotating eddies might interact to produce intense current jets and to extract filaments of cold, coastally upwelled water out to sea.

In 1986, the Coastal Transition Zone (CTZ) program [*Coastal Transition Zone Group*, 1988] was initiated with the explicit purpose of studying the structure and dynamics of the transition region, and the characteristic "filaments", "squirts", and "jets" that lie within it. The pilot phase of this project included large-scale survey cruises in winter (February 16–25 and March 19–26) and spring (May 18–27 and June 9–19) of 1987. These cruises were designed to observe the currents and water properties in the coastal transition zone over alongshore scales spanning several expected cross-shore jets. Results from these cruises are discussed below.

Once the timing of the 1987 spring transition is established (section 3 below), the development of surface fields in the coastal transition zone from winter through spring is traced using satellite and in situ data, with emphasis on the offshore extent of upwelled waters (sections 4 and 5). A meandering

[1]College of Oceanography, Oregon State University, Corvallis, Oregon.
[2]Department of Oceanography, Naval Postgraduate School, Monterey, California.
[3]Monterey Bay Aquarium Research Institute, Pacific Grove, California.
[4]Duke University Marine Laboratory, Pivers Islands, Beaufort, North Carolina.



Paper number 91JC01210.
0148-0227/91/91JC-01210$05.00

current system, continuous over long stretches of coastline, is found flowing along the front between upwelled and oceanic water in spring, transporting 2–3 Sv over the upper 200 m (sections 5 and 6); meanders in this current are shown to produce strong shoreward as well as seaward current jets (sections 5 and 6). The changes in surface properties across one such meander off Cape Mendocino are discussed in section 6. In the coastal transition zone beyond the shelf break, seasonal changes which appear to be related to upwelling are found in the mixed layer structure, in the strength of horizontal variability and in the correlation between property distributions at different depths (section 7). Examination of data from 73 conductivity-temperature-depth (CTD) stations repeated during March, May and June shows that isopycnals originally located as deep as 400 m are uplifted from winter to spring, that the magnitude of the vertical displacement was surprisingly independent of the initial isopycnal depth, and that maps of vertical isopycnal displacement resemble maps of surface properties (section 7). The cross-shore jets noted in earlier studies are thus seen to be part of a current system with substantial alongshore continuity, to be closely related to the seasonal upwelling cycle, and to carry a substantial fraction of the transport in the California Current.

## 2. DATA

The waters between 60 and 150 km off the coast of northern California formed the main sampling region for surveys. The sampling grid (Figure 1) was designed to balance the conflicting goals of sampling over long distances alongshore while maintaining acceptable synopticity. The full grid was sampled sequentially along three subgrids, each 150 km on a side, each of which took only 3 days to complete. The design included two composite alongshore transects, each

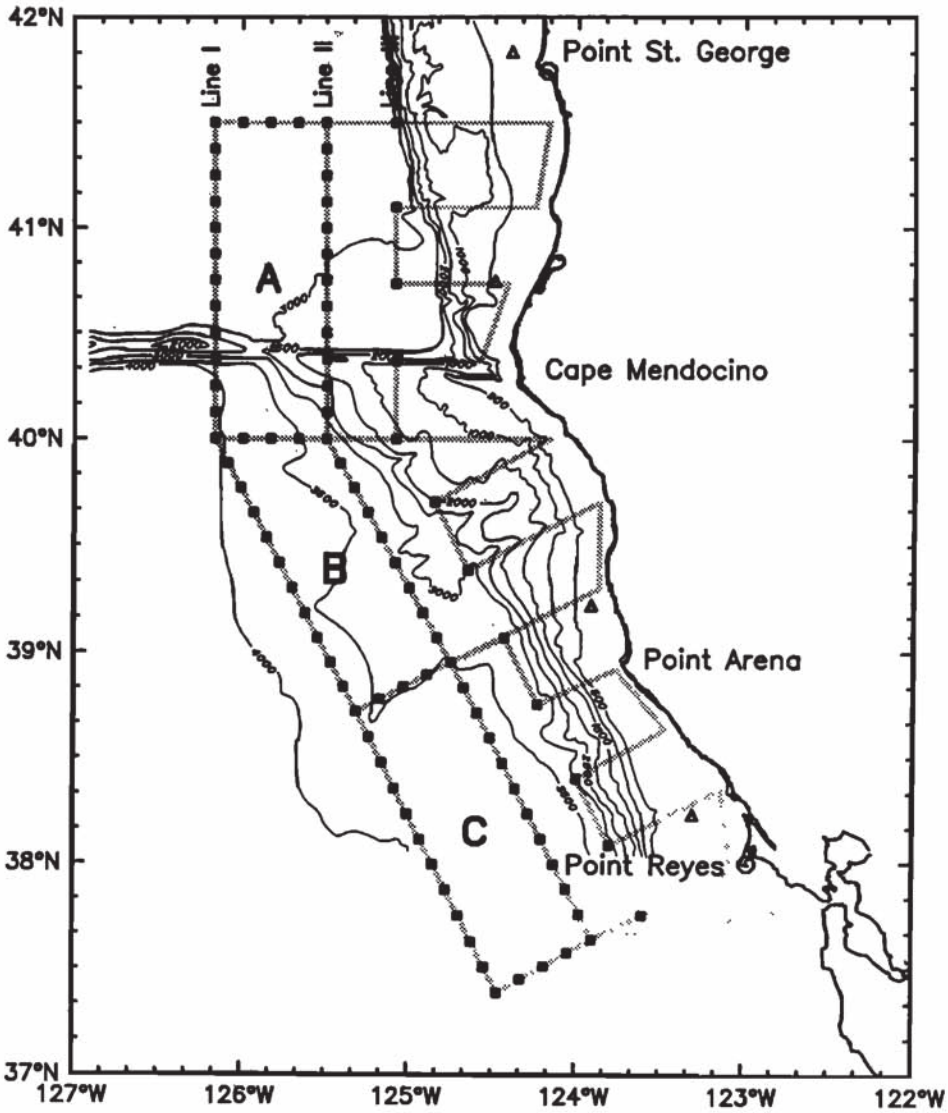


Fig. 1. The nominal station grid for the survey cruises of February 16–25, March 19–26, May 18–27 and June 9–19, 1987. Dark boxes indicate nominal CTD station positions; the light line indicates underway sampling along the ship track. Alongshore transects 150 km, 90 km and 60 km from shore are indicated as lines I, II and III respectively. The full grid was sampled sequentially as 3 smaller grids (A, B and C) each requiring about 3 days to complete. Bottom topography is shown in meters. Triangles and open circles mark the locations of the four wind buoys and two tide gauges of Figure 2.

450 km in length (lines I and II, 150 km and 90 km from shore, respectively); these were connected by four cross-shore transects to form three closed boxes. CTD stations were spaced ~15 km apart around each box. A third, discontinuous alongshore transect (line III) ran 60 km from the coast, and cross-shore transects between the shelf and 60 km or 90 km completed the station pattern. Surveys were conducted on February 16–25, May 18–27 and June 9–19 from R/V *Wecoma* and on March 19–26 from R/V *Point Sur*. Storm conditions during the February cruise restricted CTD sampling; however, near-surface measurements of temperature and salinity were collected underway over most of the grid.

A Neil Brown Mark IIIb CTD was used to measure vertical profiles of conductivity and temperature. Standard algorithms [*Fofonoff and Millard*, 1983] were used to compute derived quantities such as salinity, density, and dynamic height. A Sea Tech transmissometer (660 nm wavelength, 25 cm path length) and fluorometer were used to measure vertical profiles of optical clarity and chlorophyll fluorescence during the two spring surveys. Water samples were collected at over half the stations for calibration of the fluorometer voltage to chlorophyll-a concentration. Additional details about data processing are presented by *Schramm et al.* [1987, 1988a,b] and *Jessen et al.* [1989].

For the three *Wecoma* cruises, vertical profiles of currents, typically between 25 m and 200 m, were collected continuously along the ship's track using a 300-kHz acoustic Doppler current profiler (ADCP) manufactured by RD Instruments, with a pulse length of "12 m" (18.8 ms) and a vertical bin width of 8 m (12.6 ms). Filter skew and noise bias errors (*Chereskin et al.*, 1989) were estimated to be small (< 0.01 m/s). LORAN-C navigation data from a Trimble 100A (February) or a Northstar 5000 (May and June) receiver were used to determine absolute currents, as described by *Kosro* [1985]. The navigation data were corrected for lane jumps using the time delay data. Portions of the February data were degraded during some periods of weak signal by the presence of low-frequency errors in the positions from the Trimble receiver; data from these periods have not been used. The problem did not arise with the Northstar receiver used in May and June. A calibration error of ~1% and misalignment angle of 1.4° in the ADCP/navigation/gyrocompass system were detected from covariability between currents and ship velocity [*Kosro*, 1985; *Pollard and Read*, 1989], and then removed. Currents were estimated for each ensemble (about once per minute), and then low-pass filtered over about 30 min. For each 30-min filtering interval, short-term errors in the LORAN-C fixes were estimated from the instantaneous deviations of the ship drift away from the average; rms average errors were 68 m, 55 m and 49 m in longitude and 33 m, 36 m and 31 m in latitude during the February, May and June cruises respectively, although short-term errors occasionally exceeded 100 m. From these averages, expected rms errors in filtered currents due to LORAN-C were less than 0.05 m/s.

Underway measurements of near-surface water properties were obtained during the R/V *Wecoma* cruises. Near-surface salinity was determined using Sea-Bird sensors to measure the conductivity and temperature of filtered seawater pumped from the sea chest located in the ship's keel (5 m depth). The thermistor at the ADCP transducer face provided continuous near-surface (6 m) temperature measurements. Underway temperature and salinity were calibrated against CTD data from well-mixed stations, and against salinity from calibration samples collected at least once every 4 hours; underway salinity and temperature are considered accurate to ~0.02 psu and ~0.01°, respectively. Near-surface nutrients and chlorophyll were continuously determined from seawater streams from the ship's intake located in the bow at 3 m depth. Nitrate was measured at a horizontal resolution of roughly 200 m using reverse flow injection [*Johnson and Petty*, 1983] with a Flow Injection Sciences model ATC-30005. Chlorophyll-a concentration was measured on board ship with a Turner Designs model-10 fluorometer calibrated with commercial chlorophyll-a (Sigma). The samples for determination of plant pigments were filtered onto 25-mm Whatman GF/F filters and extracted in acetone in a freezer for between 24 and 30 hours [*Venrick and Hayward*, 1984]. Other than the modification of the extraction procedure, the method used was the conventional fluorometric procedure of *Holm-Hansen et al.* [1965].

National Data Buoy Center (NDBC) buoys 46027, 46022, 46014 and 46013 measured time series of wind speed, direction and atmospheric pressure at shelf locations offshore from Point St. George (41°50.2′N, 124°23.8′W), Eel River (40° 44.8′N, 124°29.8′W), Point Arena (39°13.3′N, 123°54.8′W) and Bodega Bay (38°13.9′N, 123°18.1′W).

Imagery of sea surface temperature from Advanced Very High Resolution Radiometer (AVHRR) sensors on NOAA-9 and NOAA-10 satellites (TIROS-N series) was collected, registered to Earth coordinates and transformed to brightness temperature by the Scripps Satellite Oceanography Facility.

Time series of subinertial variability in adjusted coastal sea level at the north and south ends of the sampling area were obtained by low-pass filtering hourly sea level data from National Ocean Service (NOS) tide gauge stations at Crescent City (41°44.7′N, 124°11.0′W) and Point Reyes (37°59.8′N, 122°58.5′W); before filtering, these data were adjusted in the usual way by removing an assumed "inverse barometer" response of sea level to fluctuations in atmospheric pressure at 1 cm/mbar. Sea level at Crescent City was adjusted using atmospheric pressure at NDBC buoys 46022 or 46027, as available; buoy 46013 was used to adjust sea level at Point Reyes.

## 3. Coastal Winds and Sea Level

The winds and coastal sea level heights observed during the times of the four cruises are highlighted in Figure 2. As expected from earlier studies [e.g., *Halliwell and Allen*, 1987), low-frequency winds were strongly polarized alongshore and were very well correlated along the coast (0.8–0.9 between adjacent buoys). Mean buoy winds were stronger in the south (−3.8 m/s at Point St. George, −3.1 m/s at Eel River, −4.9 m/s at Point Arena and −5.9 m/s at Bodega Bay, for the common data period from March 22 to June 30); low-frequency fluctuations ranged from 3.2 m/s standard deviation at Eel River to 5.0 m/s at Point St. George.

During February and mid-March, both strongly upwelling-favorable (equatorward) and downwelling-favorable (poleward) wind events were observed. Coastal sea level dropped over 0.3 m in response to strong upwelling-favorable winds in mid-February, but rose to former levels as winds reversed

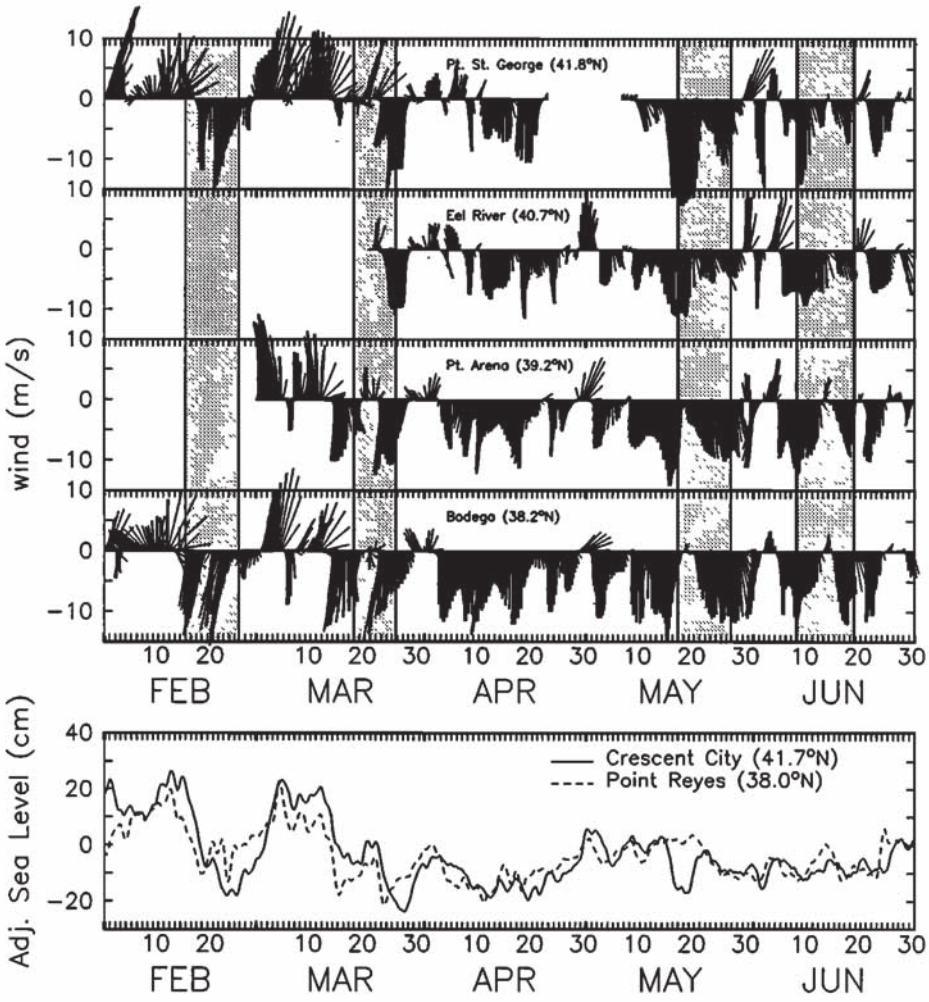


Fig. 2. (Top) Winds measured over the shelf at NDBC buoys 46027, 46022, 46014 and 46013 offshore from Point St. George (41°50.2′N, 124°23.8′W), Eel River (40°44.8′N, 124°29.8′W), Point Arena (39°13.3′N, 123°54.8′W) and Bodega Bay (38°13.9′N, 123°18.1′W), respectively. Data have been low-pass filtered using a 40-hour half-power point, and rotated clockwise by 20°, 0°, 35°, and 55° respectively. Highlighted periods correspond to surveys (February 16–25, March 19–26, May 18–27, June 9–19, 1987). Lower panel: Sea-level from NOS tide gauges at Crescent City (41°44.7′N, 124°11.0′W) and Point Reyes (37°59.8′N, 122°58.5′W), adjusted for inverse barometer response using atmospheric pressure from nearby NDBC buoys (46013 for Point Reyes, 46027 for Crescent City except during April 23 to May 7, when 46022 was used), and filtered as with winds.

in early March. From mid-March through August, upwelling-favorable winds strongly predominate. Beginning about March 14, the onset of strong upwelling-favorable winds in the south was accompanied by a persistent drop in sea level at Point Reyes (38.0°N). Sea level at Crescent City (41.7°N) dropped a comparable amount, even though upwelling-favorable winds were not yet seen at the nearby NDBC buoy 46027. A second episode of strong upwelling-favorable winds began all along the coast on March 23, accompanied by a further drop in sea level at the northern station.

From these data, it appears that the spring transition to sustained upwelling conditions [*Huyer et al.*, 1979; *Strub et al., 1987*; *Lentz*, 1987] occurred in mid-March, near the start of the March cruise (Figure 2). Therefore, although the wind forcing during each cruise was similar, the May and June surveys should reflect a more mature stage of the spring upwelling circulation than the February and March surveys; we will call the latter "winter" surveys.

## 4. SURFACE FIELDS IN THE TRANSITION ZONE

The growth of the upwelling and transition zones from winter through spring and summer is indicated by the montage of satellite AVHRR imagery of sea surface temperature in Figure 3. The earliest winter image, from February 5, showed low contrast in surface temperature, with no consistent cross-shore gradient. By February 25, following nearly a week of very strong upwelling-favorable winds (Figure 2), a band of cold, upwelled water could be seen within about 25 km of the coast. This band widened considerably south of Cape Mendocino and offshore from Point Arena and Point Reyes. Downwelling favorable winds dominated in early March, and the upwelling zone appears to have retreated to a narrow coastal strip by March 19. By May 5, narrow filaments of cold water could be seen projecting from each of the three major coastal points: Cape Mendocino, Point Arena and Point Reyes. Each filament curled back toward the coast further to the south. In May, the filament

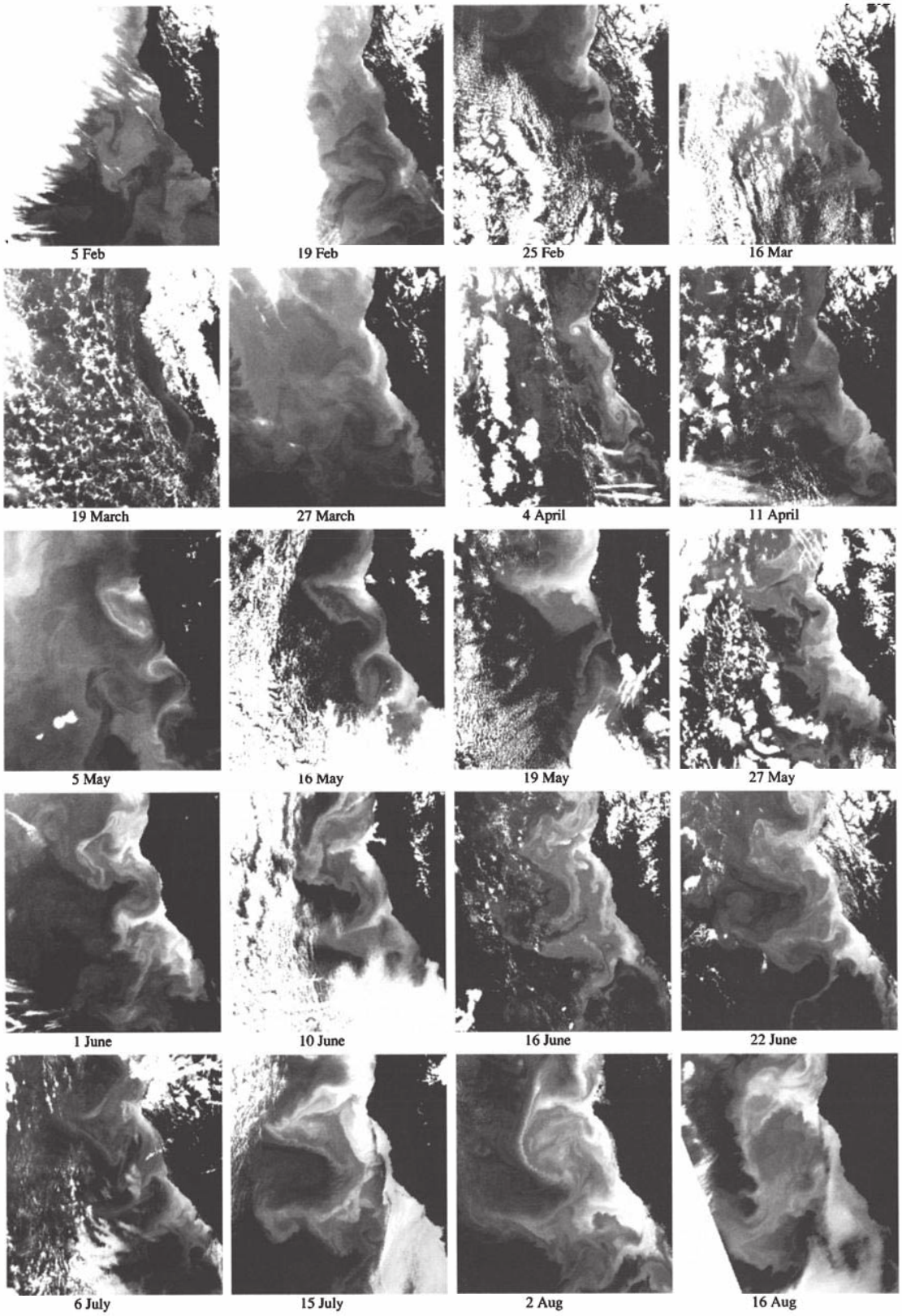


Fig. 3. Satellite (NOAA-9, TIROS-N series) AVHRR infrared images of brightness temperature in the survey region between 41.5°N and 36.5°N for the period February 5 to August 16, 1987. Each image has been enhanced to emphasize ocean features in the coastal and transition zones. No cloud masking has been performed for any of the images. Lighter shades indicate colder brightness temperatures.

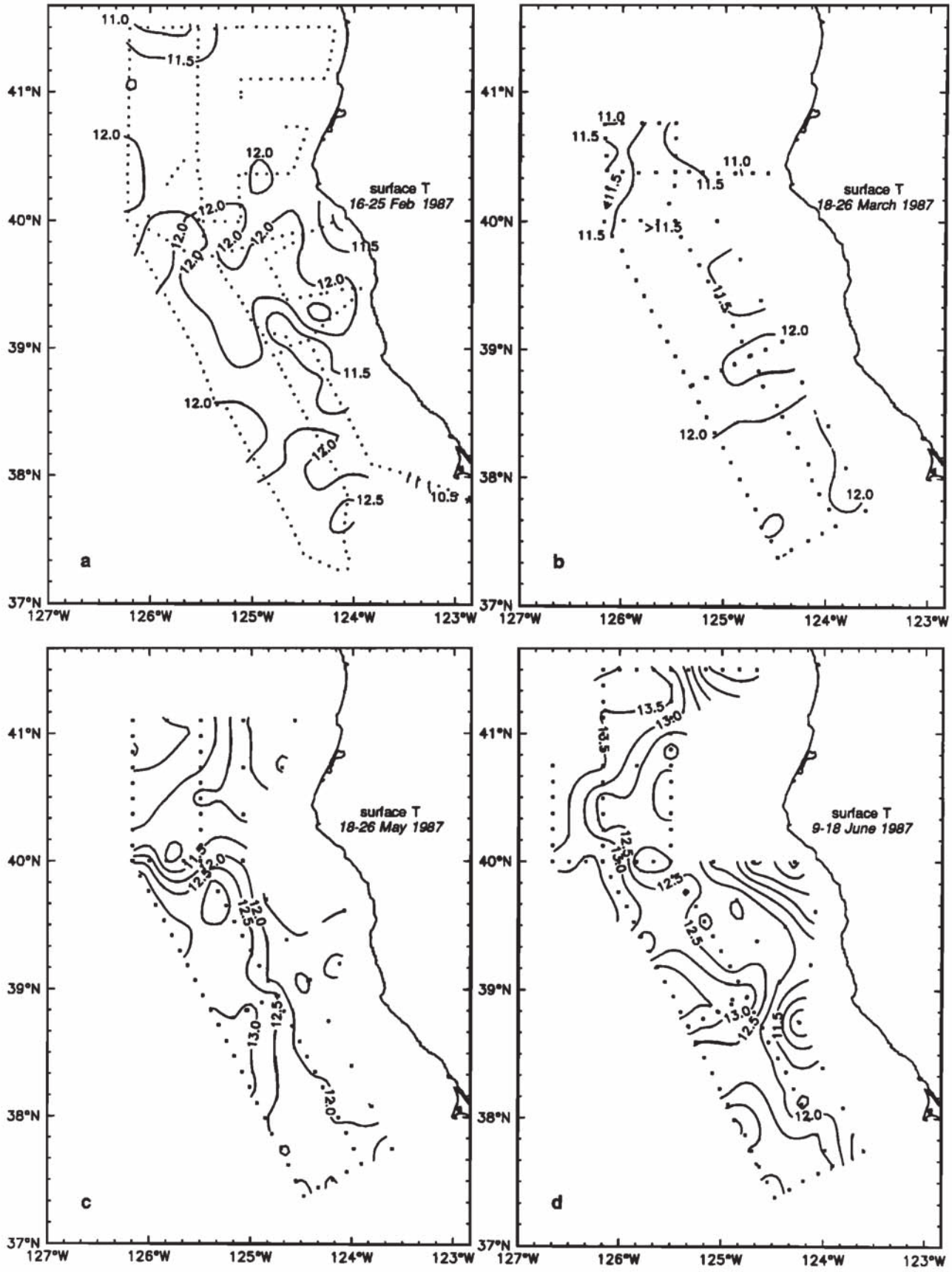


Fig. 4. Surface temperature (°C) for each cruise, objectively mapped from values at station locations (indicated by dots): (*a*) February, (*b*) March, (*c*) May, (*d*) June. Station values are from CTD casts (March, May and June) or spatially averaged underway thermosalinograph (February).

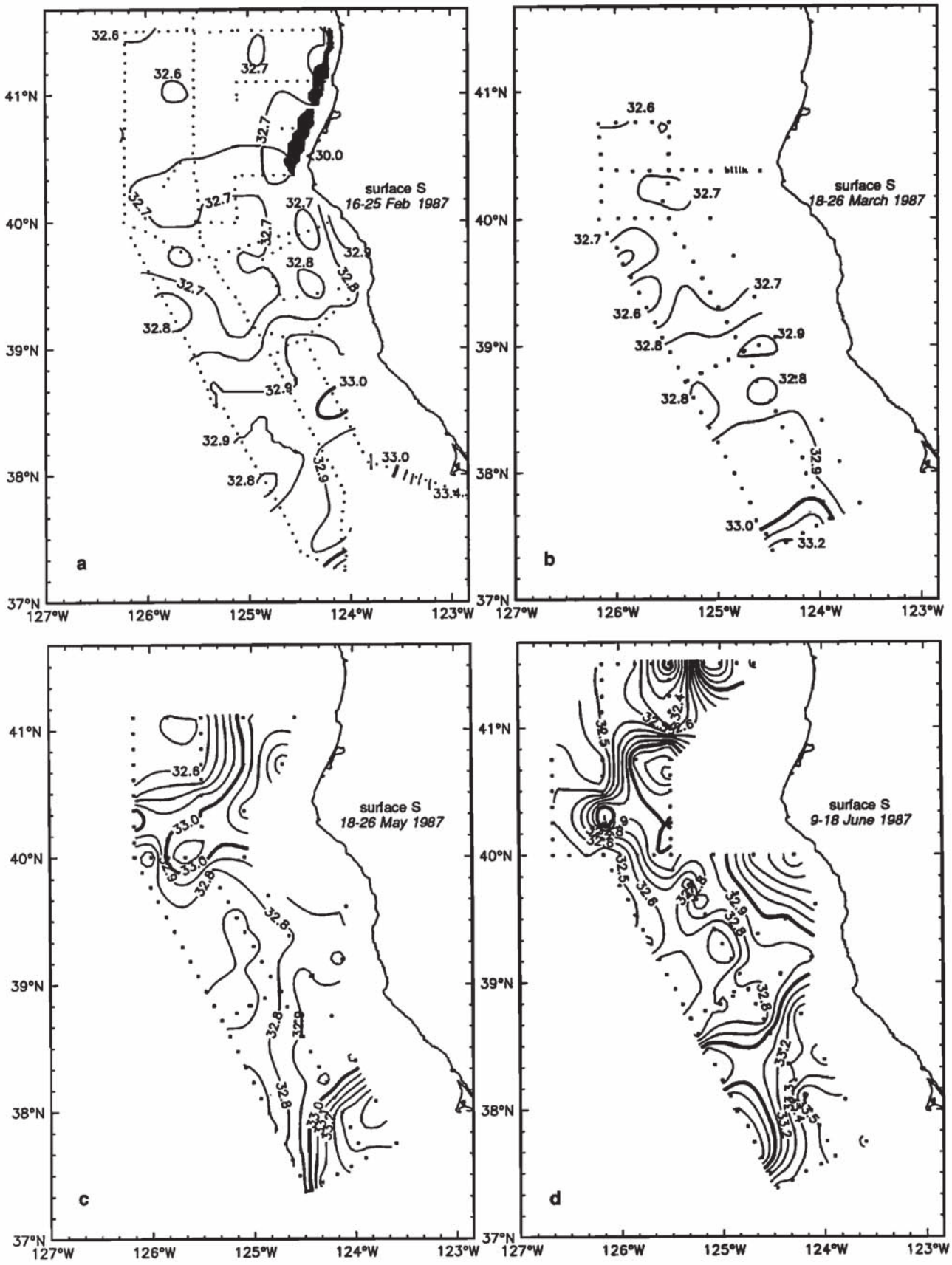


Fig. 5. Surface salinity (psu) for each cruise, as in Figure 4: (*a*) February, (*b*) March, (*c*) May, (*d*) June.

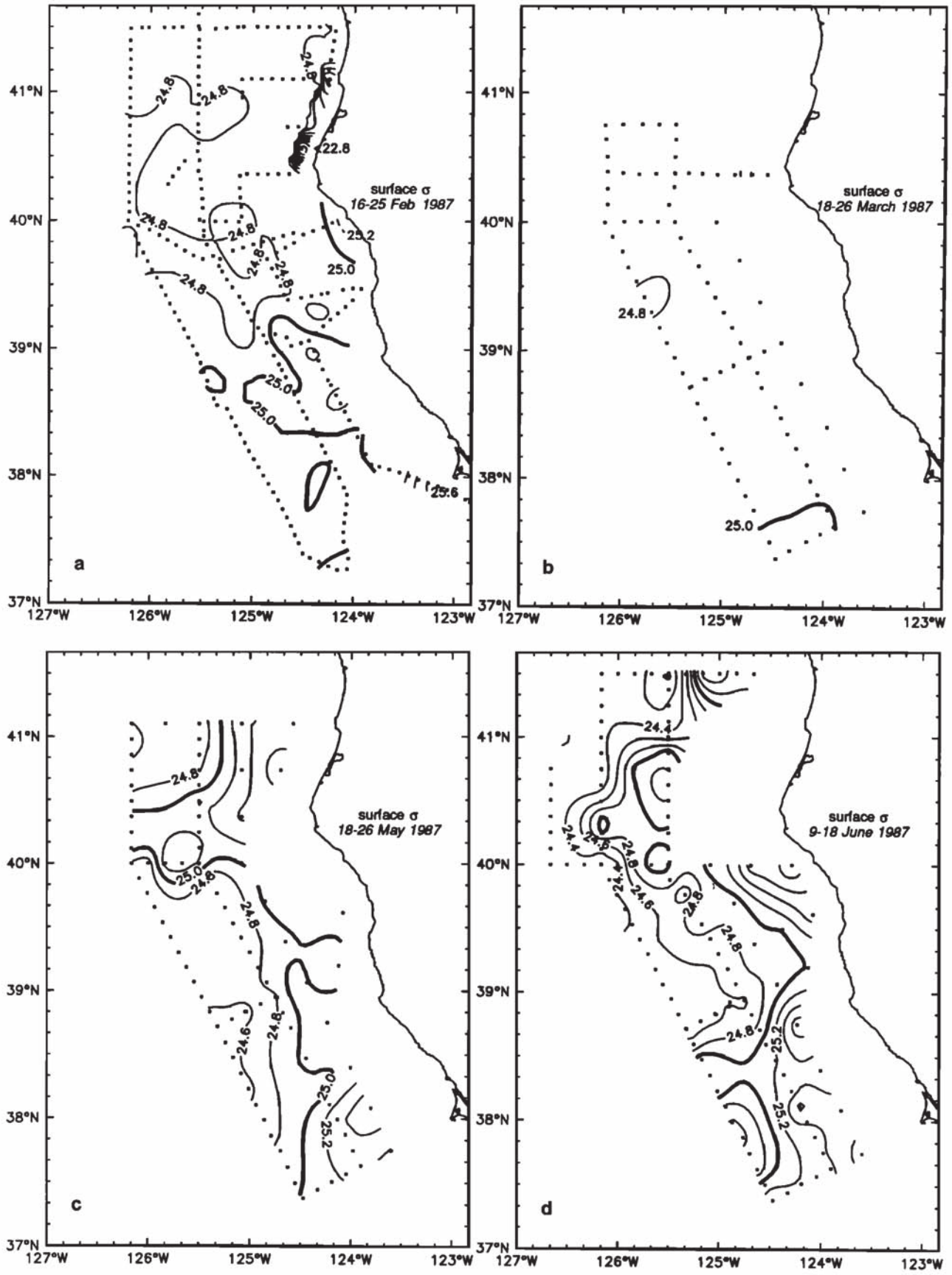


Fig. 6. Surface density anomaly $\sigma_t$ (kg/m$^3$) for each cruise, as in Figure 4: (*a*) February, (*b*) March, (*c*) May, (*d*) June.

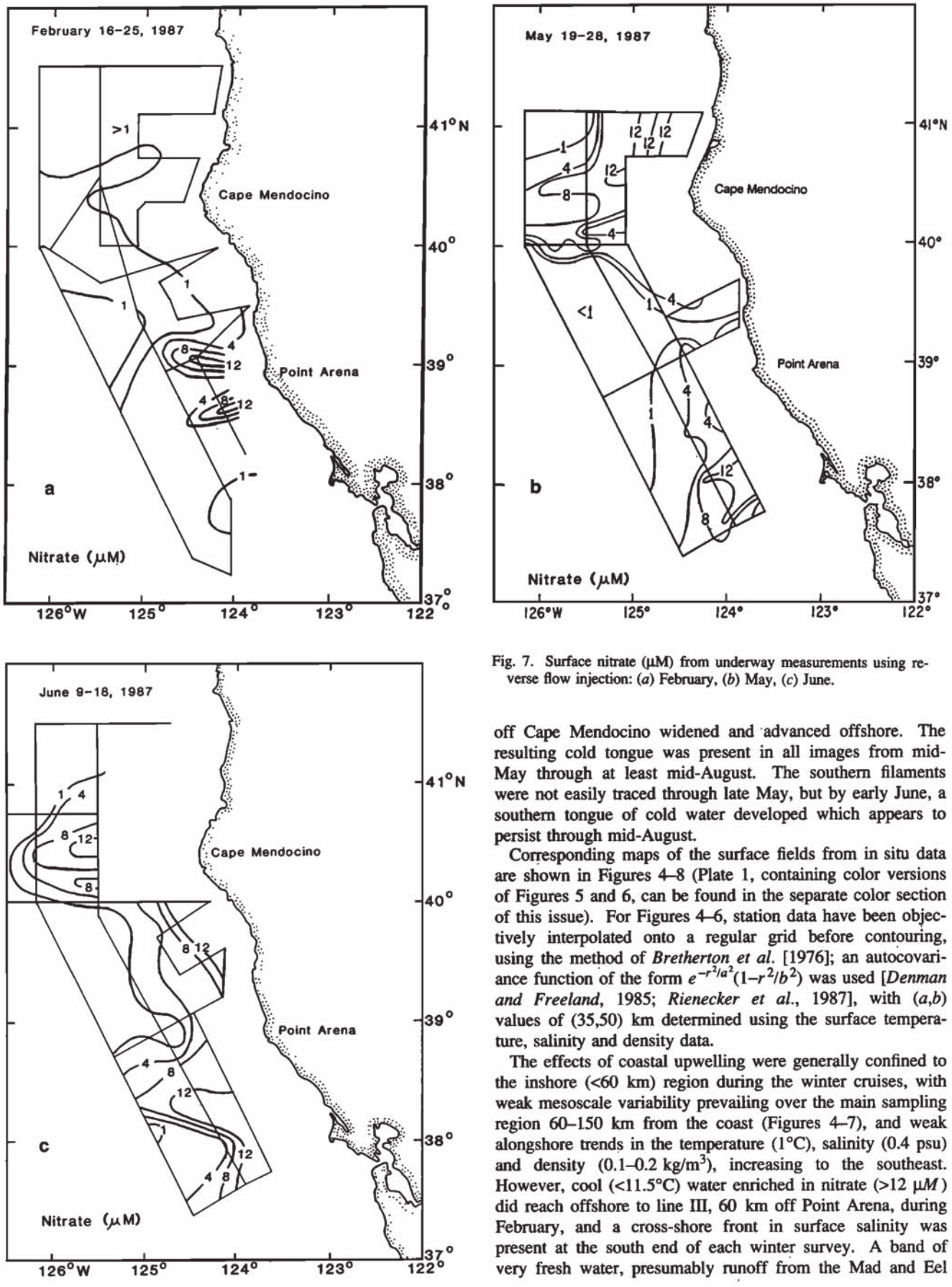


Fig. 7. Surface nitrate (μM) from underway measurements using reverse flow injection: (*a*) February, (*b*) May, (*c*) June.

off Cape Mendocino widened and advanced offshore. The resulting cold tongue was present in all images from mid-May through at least mid-August. The southern filaments were not easily traced through late May, but by early June, a southern tongue of cold water developed which appears to persist through mid-August.

Corresponding maps of the surface fields from in situ data are shown in Figures 4–8 (Plate 1, containing color versions of Figures 5 and 6, can be found in the separate color section of this issue). For Figures 4–6, station data have been objectively interpolated onto a regular grid before contouring, using the method of *Bretherton et al.* [1976]; an autocovariance function of the form $e^{-r^2/a^2}(1-r^2/b^2)$ was used [*Denman and Freeland*, 1985; *Rienecker et al.*, 1987], with (*a*,*b*) values of (35,50) km determined using the surface temperature, salinity and density data.

The effects of coastal upwelling were generally confined to the inshore (<60 km) region during the winter cruises, with weak mesoscale variability prevailing over the main sampling region 60–150 km from the coast (Figures 4–7), and weak alongshore trends in the temperature (1°C), salinity (0.4 psu) and density (0.1–0.2 kg/m$^3$), increasing to the southeast. However, cool (<11.5°C) water enriched in nitrate (>12 μ*M*) did reach offshore to line III, 60 km off Point Arena, during February, and a cross-shore front in surface salinity was present at the south end of each winter survey. A band of very fresh water, presumably runoff from the Mad and Eel

Rivers, was present near Cape Mendocino in both February and March.

The surface fields 60–150 km from the coast showed much stronger horizontal variation during the spring cruises, with the effects of upwelling being both more pronounced and widespread (Figures 4–8). Measurements in spring showed cooler, saltier surface water present inshore and warmer, fresher water present offshore than were found during winter. The warm, fresh water far from shore showed minimum concentrations of surface nitrate and chlorophyll, while enhanced concentrations (peak values >30 $\mu M$ $NO_3$ and >20 mg/m$^3$ chlorophyll) were associated with high density surface water (Figure 9), indicative of upwelling.

At the northern boundary of each spring survey, a strong salinity front and a moderate temperature front were present between lines II (90 km offshore) and III (60 km offshore);

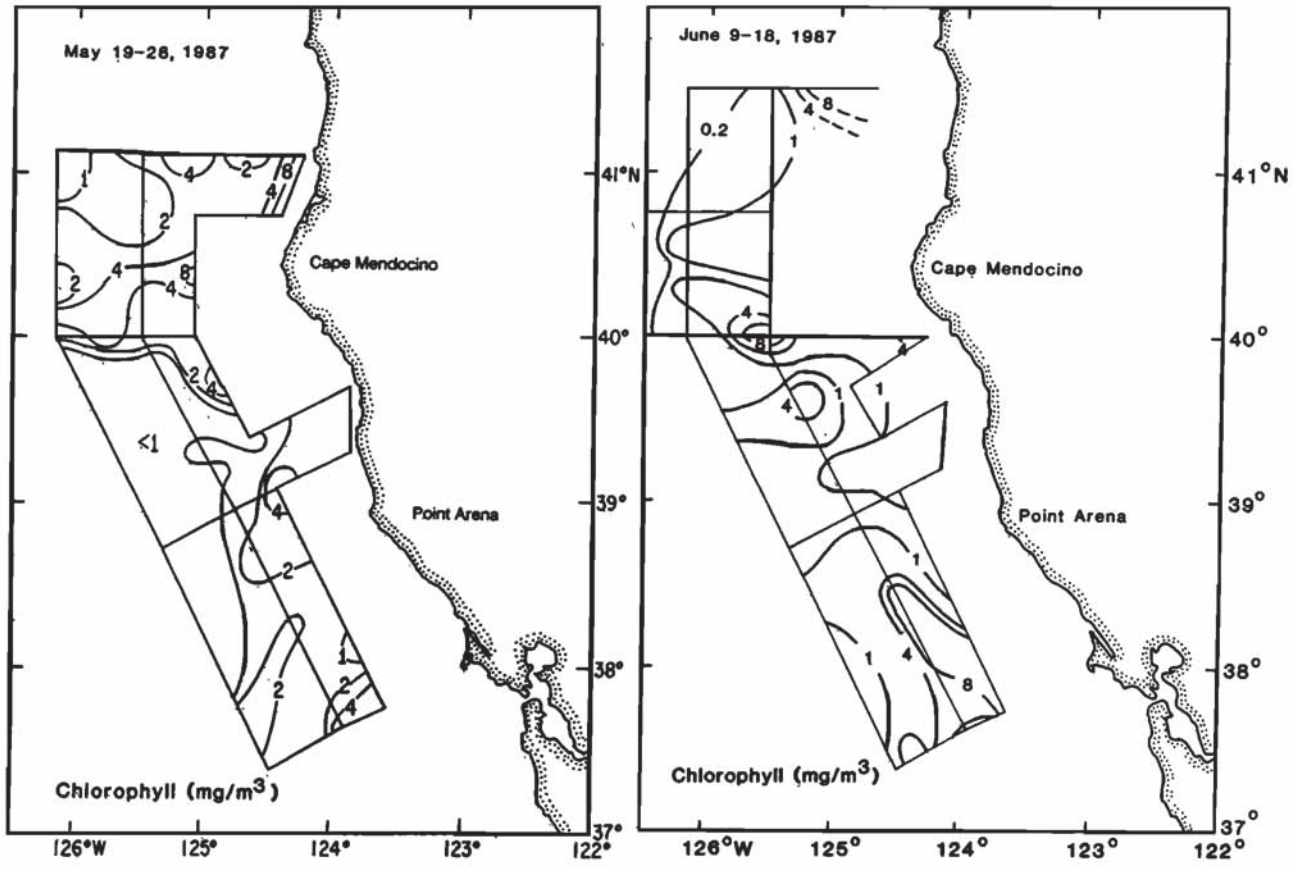


Fig. 8. Surface chlorophyll (mg/m$^3$), from extraction of bottle samples.

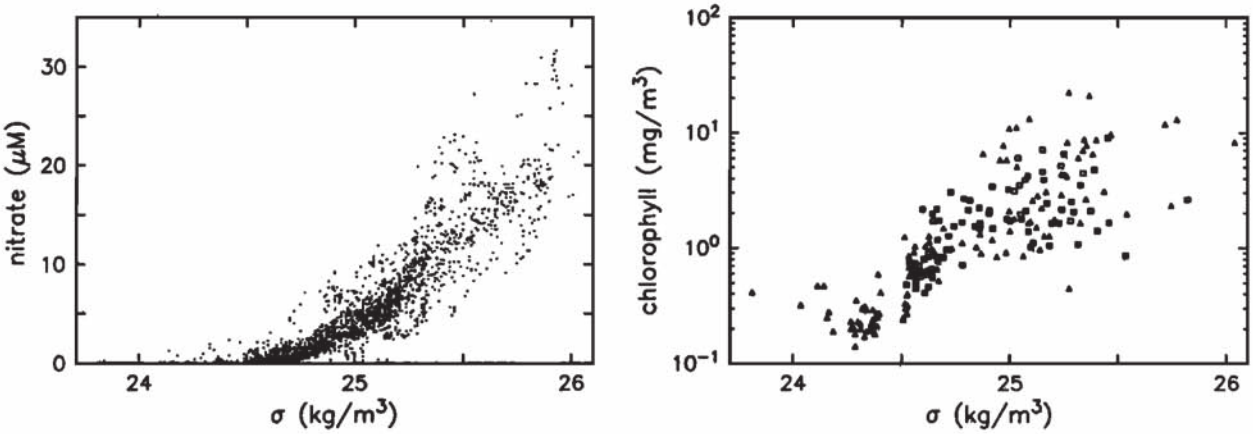


Fig. 9. (Left) Surface nitrate (μM) from underway measurements and (right) surface chlorophyll from bottle samples, both plotted against surface density anomaly $\sigma_t$ (kg/m$^3$). Data are from the May and June cruises only.

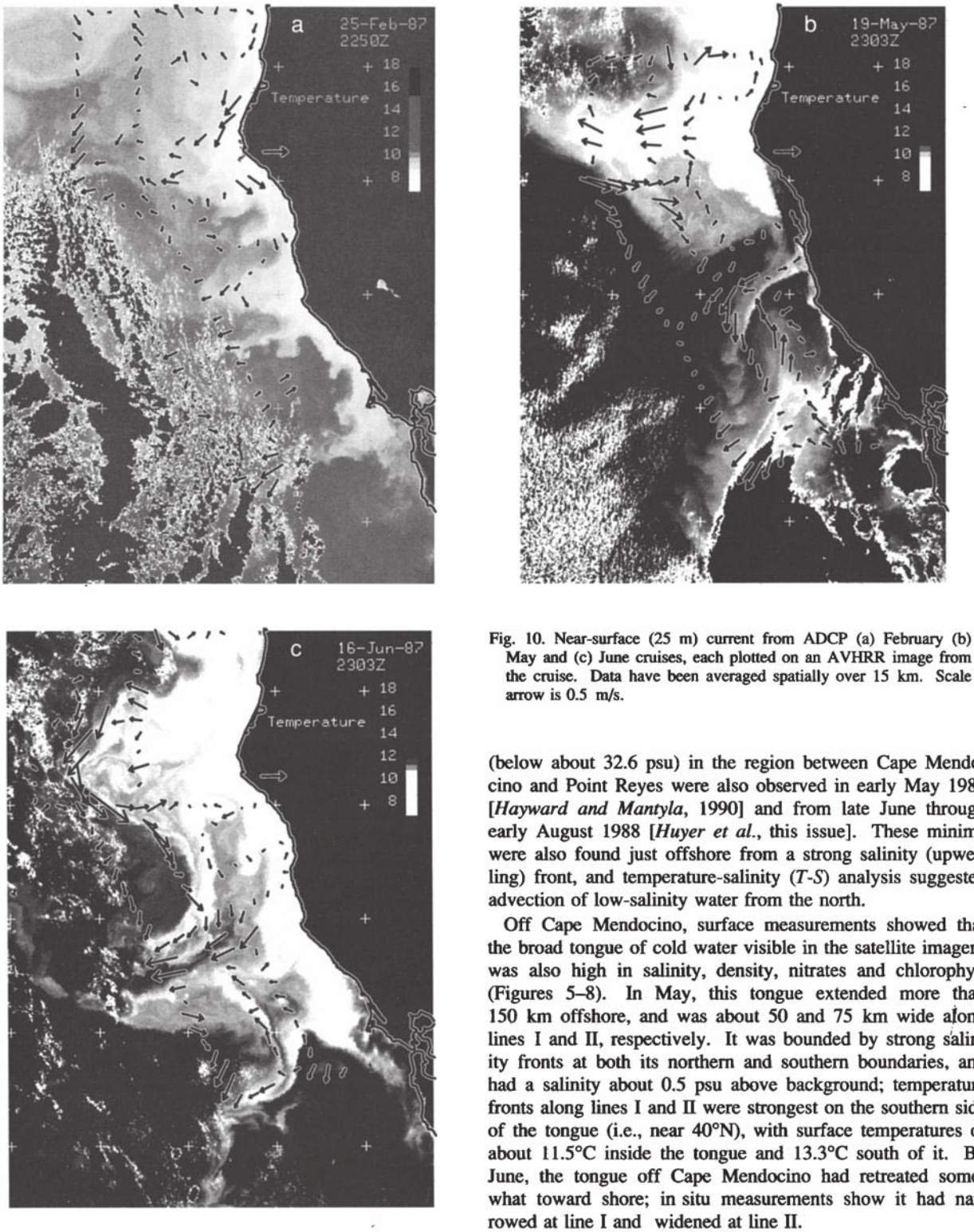


Fig. 10. Near-surface (25 m) current from ADCP (a) February (b) May and (c) June cruises, each plotted on an AVHRR image from the cruise. Data have been averaged spatially over 15 km. Scale arrow is 0.5 m/s.

in June, surface density changed by 1 kg/m$^3$ across this front, and surface chlorophyll exceeded 8 mg/m$^3$ just inshore of it. This front, 60–90 km offshore and well beyond the shelf break, appears to mark the boundary between coastally upwelled and offshore water. Salinity minima were found just offshore of this front in both surveys. Salinity minima (below about 32.6 psu) in the region between Cape Mendocino and Point Reyes were also observed in early May 1987 [*Hayward and Mantyla*, 1990] and from late June through early August 1988 [*Huyer et al.*, this issue]. These minima were also found just offshore from a strong salinity (upwelling) front, and temperature-salinity ($T$-$S$) analysis suggested advection of low-salinity water from the north.

Off Cape Mendocino, surface measurements showed that the broad tongue of cold water visible in the satellite imagery was also high in salinity, density, nitrates and chlorophyll (Figures 5–8). In May, this tongue extended more than 150 km offshore, and was about 50 and 75 km wide along lines I and II, respectively. It was bounded by strong salinity fronts at both its northern and southern boundaries, and had a salinity about 0.5 psu above background; temperature fronts along lines I and II were strongest on the southern side of the tongue (i.e., near 40°N), with surface temperatures of about 11.5°C inside the tongue and 13.3°C south of it. By June, the tongue off Cape Mendocino had retreated somewhat toward shore; in situ measurements show it had narrowed at line I and widened at line II.

South of 39°N, a second wedge of high-salinity, high-nutrient, high-chlorophyll surface water was present in both surveys. In May, the strong surface salinity front at the northern edge of the wedge crossed lines II and III north of Point Reyes and passed through the southwest corner of the grid. By mid-June, a tongue extending across line I, with surface salinities reaching 33.19, had developed.

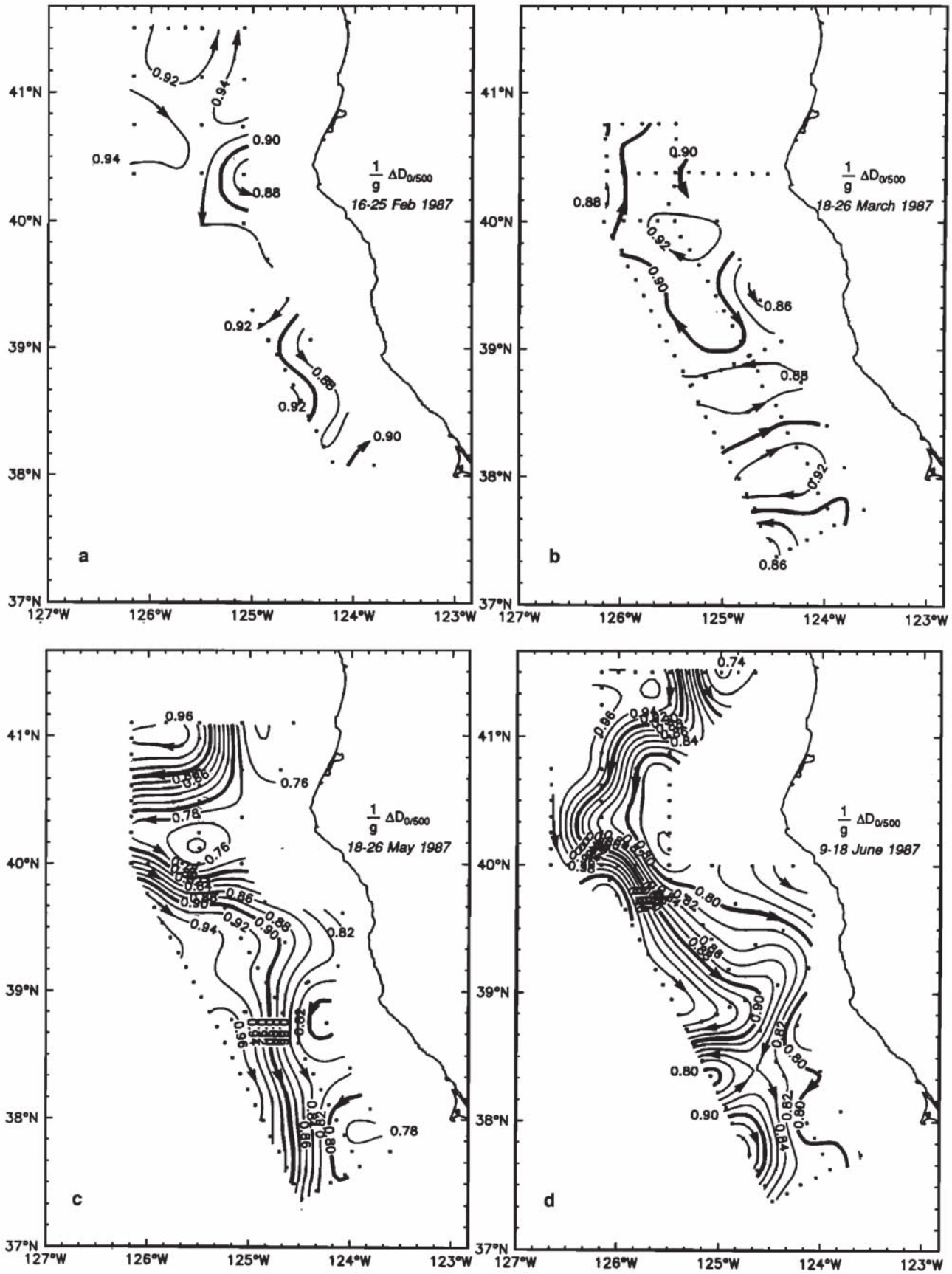


Fig. 11. $\Delta D_{0/500}/g$ (meters), the dynamic height of the sea surface relative to 500 dbar, here normalized by the acceleration of gravity, for (*a*) February, (*b*) March, (*c*) May, (*d*) June.

## 5. NEAR SURFACE FLOW IN THE TRANSITION ZONE

The near-surface flow field associated with these features was obtained both from direct measurements, using the ship-borne ADCP (Figure 10), and from the dynamic topography of the sea-surface relative to 500 dbar, $\Delta D_{0/500}$ (Figure 11, Plate 1). The correlation scales of $\Delta D_{0/500}$ were determined to be longer than those of surface $T$, $S$, and $\sigma_t$; $\Delta D_{0/500}$ was objectively mapped using an autocovariance function of the form $e^{-r^2/a^2}(1-r^2/b^2)$ with $(a,b)$ values of (50,70) km.

During the winter surveys, measured variations of $\Delta D_{0/500}$ were weak in the main sampling region (Figures 11*a* and 11*b*). Despite strong wind forcing and strong sea level response at the coast (Figure 2), measurements of $\Delta D_{0/500}$ varied by less than 0.1 m over the main sampling region 60–150 km from the coast; in February, $\Delta D_{0/500}$ indicated a weak (~0.2 m/s) cyclonic flow off Cape Mendocino and weak equatorward flow past Point Arena, and in March, the surface topography indicated anticyclonic flow around two broad, gentle peaks centered near 38.0°N, 124.5°W and near 40.0°N, 125.5°W. In February, directly measured near-surface currents were available over a larger region than for $\Delta D_{0/500}$ (Figure 10*a*); these were strongest inshore of the main sampling region, where an alongshore coastal current was present over the shelf and inner slope between 41.5°N and 39.5°N, and at about 100 km off Point Reyes, where a seaward current flowed along the salty side of the salinity front seen in Figure 5*a*; 15 km averages of both currents registered up to 0.5 m/s. Aircraft-tracked surface drifters deployed in the Northern California Coastal Circulation Study [*Magnell et al.*, 1990] also indicated an alongshore coastal current during March 13–24, with most of the drifters remaining within 50 km of the coast.

The near-surface currents were considerably stronger in spring. The largest current speeds observed in spring were ~1 m/s, and the kinetic energy in the spring current maps was about twice that in the winter map, with speeds averaging 0.27 m/s in spring and 0.20 m/s in winter. In May, the cold tongue off Cape Mendocino was associated with two cross-shore current jets (Figure 10). North of Cape Mendocino, the offshore-directed jet crossed both lines I and II along 40.5°N, extending offshore beyond the sampling region, and showed peak speeds of 0.7 m/s (averaged over 15 km). The onshore-directed jet, with even higher peak speeds of 0.9 m/s (averaged over 15 km) returned across lines I and II along 40.0°N. The offshore flow north of Cape Mendocino and onshore flow farther south were still present across line II in June, but the currents on line I had developed a strong alongshore component, so that the feature seemed to be a gentle meander in a southward flowing current. Strong cross-shore currents across lines II and III were also observed in June off Point Arena, as well as through the southwest corner of the grid off Point Reyes. Between May and June, a second pair of cross-shore current jets developed across line I off Point Arena near 38.5°N, 125.0°W, flanking the tongue of cold, high-salinity

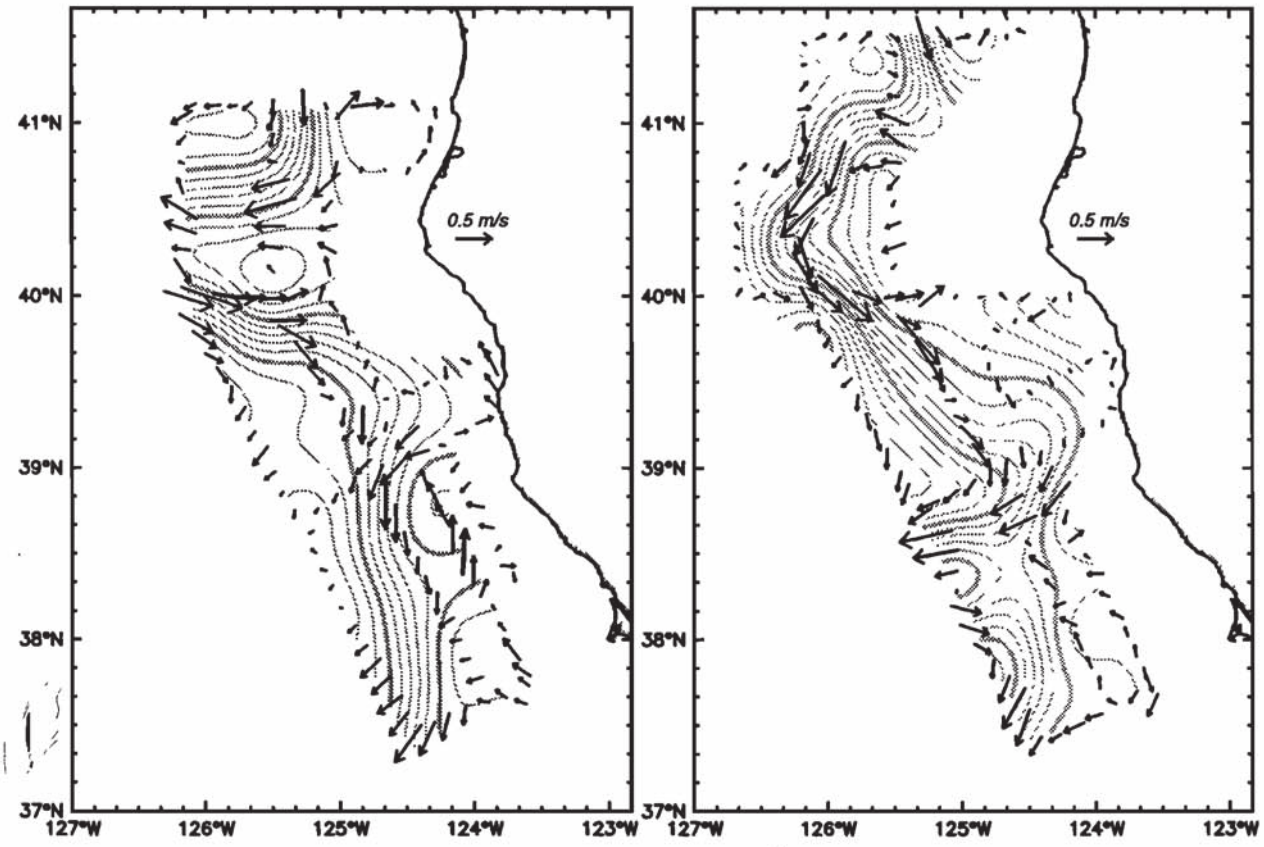


Fig. 12. ADCP current vectors from 25 m for the (left) May and (right) June cruises, superimposed on contours of $\Delta D_{25/500}$. Contour interval is 0.02 m.

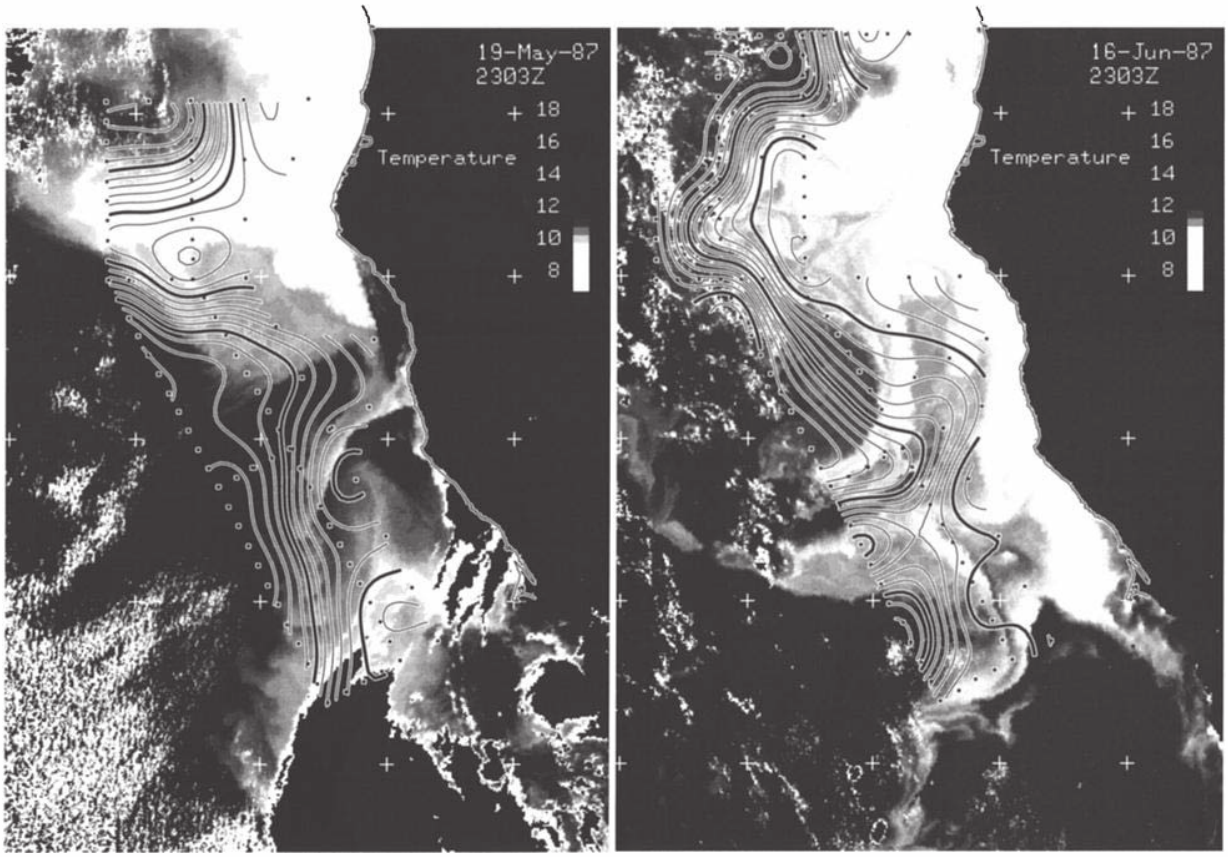


Fig. 13. Contours of $\Delta D_{0/500}/g$ for the (left) May and (right) June cruises, plotted over satellite AVHRR images. Contour interval is 0.02 m.

water which developed there; as off Cape Mendocino, offshore flow was associated with the northern flank of the tongue and onshore flow with its southern flank. Direct measurements showed that the flow was northward in May along line III below Point Arena.

The connection between these currents is highlighted by $\Delta D_{0/500}$, which clearly showed an equatorward-tending current, continuous over hundreds of kilometers alongshore, flowing along the meandering boundary between low and high steric sea levels during these spring cruises (Figure 11). The core of the current lay more than 100 km from shore at some locations. The cross-shore jet pairs off Cape Mendocino (May and June) and Point Arena (June) were associated with troughs of 0.15–0.20 m in steric sea level. Low sea level to the left of the current tended to be associated with cold, salty upwelled surface water; the correlation between $\Delta D_{0/500}$ and surface $T$, $S$ and $\sigma_t$ were 0.69, -0.77 and -0.87, respectively, in May and 0.81, -0.75 and -0.84 in June.

The directly measured currents were generally well aligned with $\Delta D_{0/500}$ (Figure 12). However, the strong northward flow seen in the May ADCP measurements along line III between 38°N and 39°N, sometimes exceeding 0.5 m/s, was not resolved in $\Delta D_{0/500}$. Advection of cold surface water by this branch of the flow is evident in the surface AVHRR data from May 19 (Figures 3 and 10). Mixed-layer drifters [Paduan and Niiler, 1990] also traced this poleward flow to about 38.7°–38.9°N (off Point Arena) before turning offshore and then being carried equatorward in the flow observed along line II. Below 50 m, the vertical shear in the poleward current was generally weak, with measured currents at 200 m often exceeding 0.2 m/s northward. *Walstad et al.* [this issue] discuss the effect which resolving the poleward branch of the current had in improving the evolution of their quasigeostrophic model.

The tendency for a strong current to be found near the upwelling front, with warmer (and fresher) water to the right of the current, is seen when the 25-m ADCP currents and $\Delta D_{0/500}$ are superimposed on the satellite AVHRR images (Figures 10 and 13).

## 6. JET TRANSECTS

Several crossings of current jets were made during the spring surveys. The subsurface structure observed on six jet crossings is given in Figures 14 (two crossings) and 15 (four crossings) which show, respectively, east-west sections through the equatorward flow past 41.5°N and 40.0°N in June, and north-south sections through the pair of jets flowing offshore and onshore past lines I and II off Cape Mendocino in May. The zonal transect along 41.5°N crossed the strong front in temperature and salinity about 100 km from the coast (Figure 14). Isotherms and isohalines rose by 50 m or more toward the coast across this front, reinforcing the idea that the front was formed during coastal upwelling. Quite similar changes were encountered on the other five frontal crossings, except that the alongshore front was located 160 km from shore at 40.0°N, and the zonal fronts were

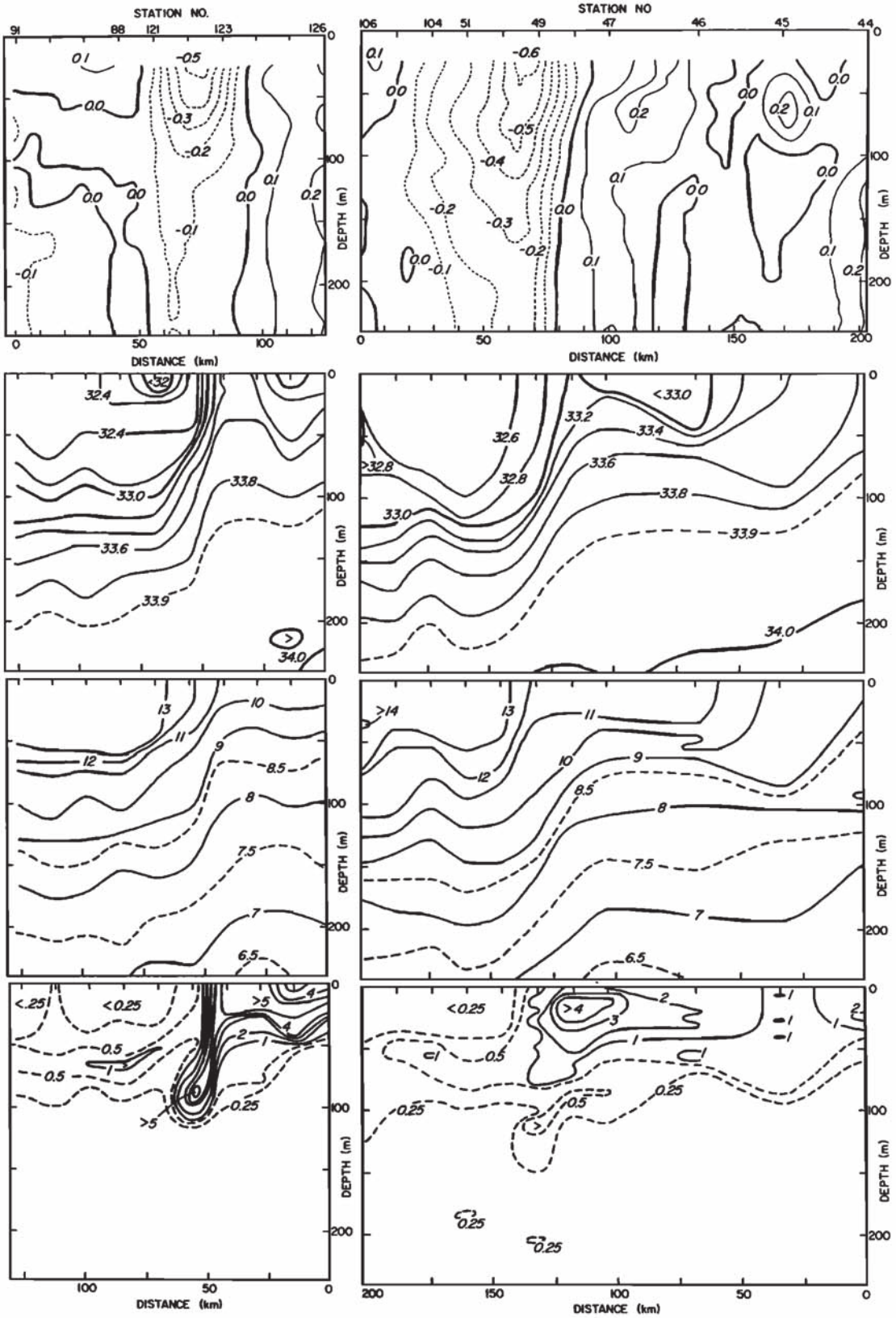


Fig. 14. Vertical sections of the normal velocity component, salinity, temperature and fluorescence for east-west sections along (left) 41.5 °N and (right) 40.0 °N through the current in June 1987. East is on the right.

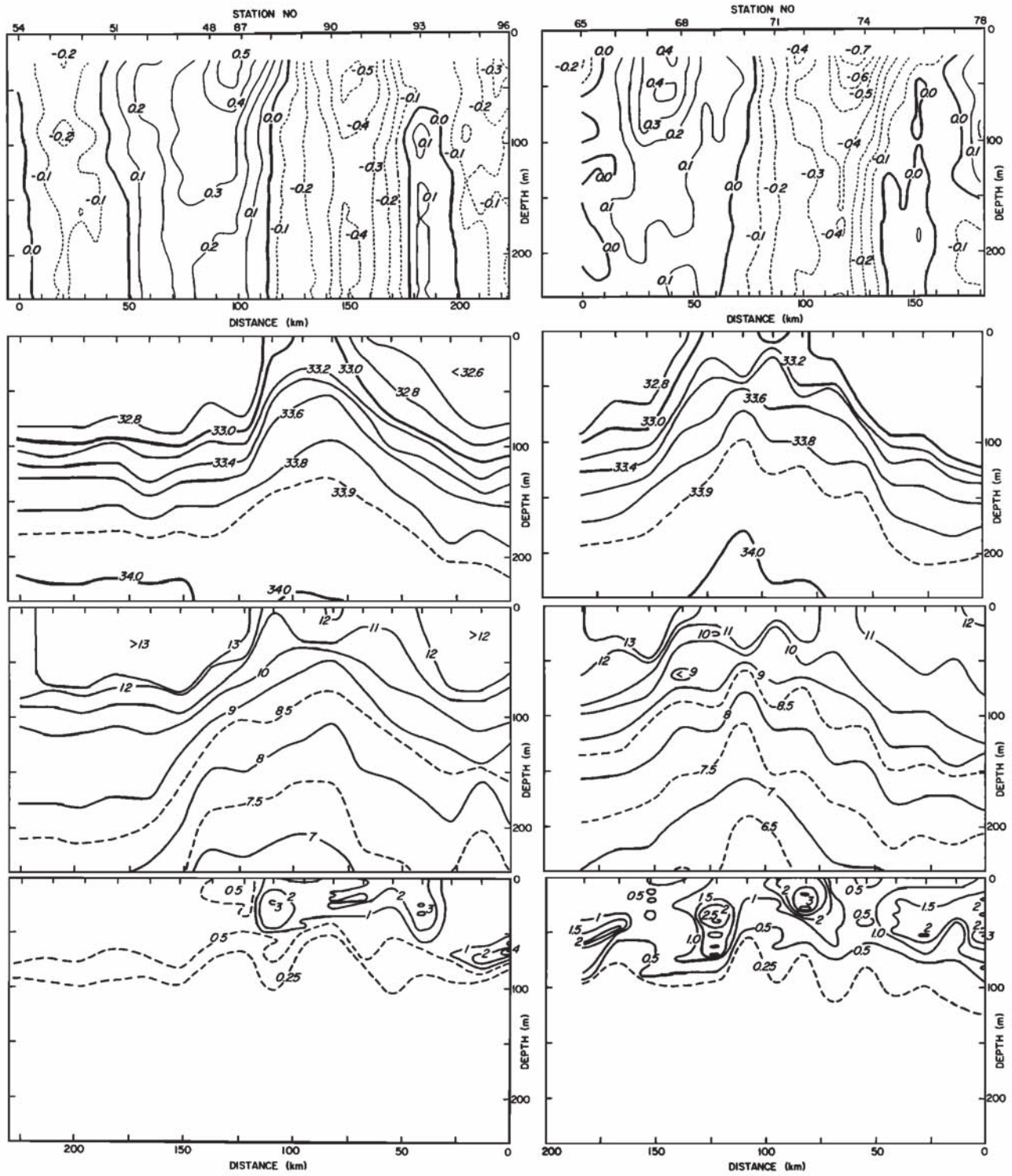


Fig. 15. Vertical sections of the normal velocity component, salinity, temperature and fluorescence for alongshore transects along lines (left) 150 km and (right) 90 km from shore through the meander off Cape Mendocino in May 1987. North is on the right; stations 87 (left) and 69 (right) each are at 40°N.

crossed in pairs, with the cold, high salinity upwelled water located between them (Figures 14 and 15).

A current jet about 30–50 km wide was found on each of the six frontal crossings; core currents had cross-transect components ranging from 0.5 to 0.8 m/s. In each crossing, the current jet was appreciably sheared over the upper 100 m, yet the current at 100–150 m depth exceeded 0.3 m/s in most cases. Between the oppositely directed zonal jets, horizontal changes in current persisted vertically, with only weak vertical shear over the upper 200 m. The jets were directed equatorward on two crossings, offshore on two, and onshore on two. The average transport over the

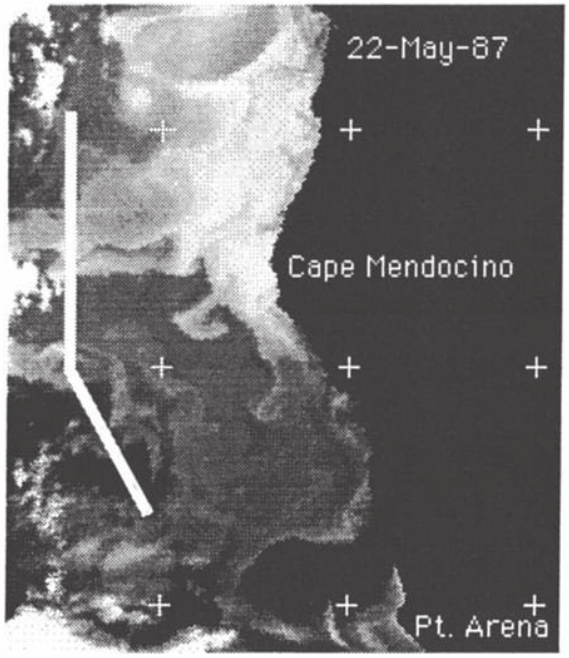


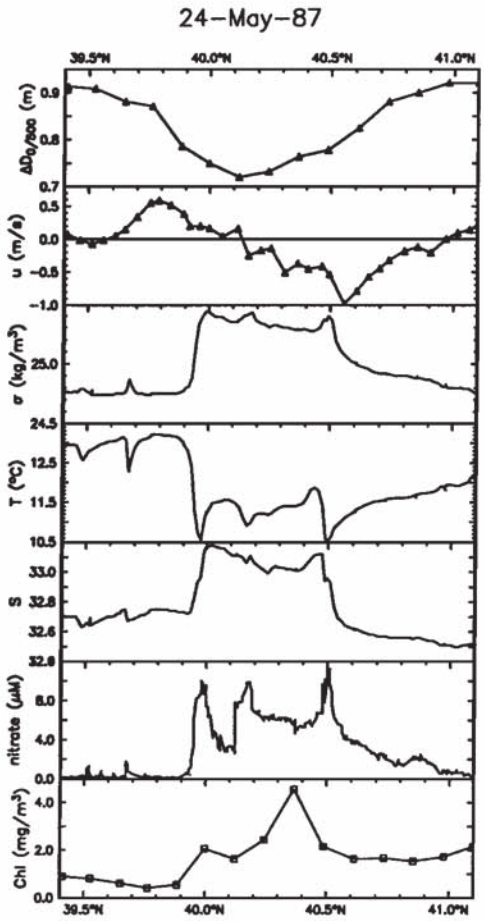


Fig. 16. At right, values of near-surface variables on a cross-plume transect from May 24, 1987 (dynamic height $\Delta D_{0/500}/g$ (m), eastward current measured with the ADCP (m/s), density anomaly $\sigma_t$ (kg/m$^3$), temperature (°C), salinity (psu), nitrate $NO_3$ (μM), and chlorophyll-a measured by extraction (mg/m$^3$)). At left, ship track is plotted over AVHRR image for May 22, (note the 1- to 2-day lag between the satellite and ship data).

upper 200 m was 3.2 ± 1.0 Sv from direct measurements (mean ± standard deviation) and 2.0 ± 0.3 Sv from geostrophy, using a 500-dbar reference level. The observed similarity of structure among the various frontal and jet crossings supports the suggestion that the alongshore jet which entered the region at 41.5°N was continuous with both the offshore-flowing and onshore-flowing jets which straddled Cape Mendocino, and that the jets occurred along a front formed during coastal upwelling.

Patchy enhancement of chlorophyll levels within the surface layer could be seen inshore of the upwelling front in June (Figure 14), and in the cold, high-salinity tongue off Cape Mendocino in May (Figure 15). A maximum in chlorophyll fluorescence was centered quite deep (near 90 m) in June near the upwelling front along 41.5°N (Figure 14); a corresponding minimum in light transmission was also present [*Schramm et al.*, 1988b]. Biological evidence that such deep maxima were formed by the subduction of near-surface water is discussed in detail by *Hood et al.* [this issue] and *Washburn et al.* [this issue].

The detailed relationship among surface features encountered on one crossing of the meander off Cape Mendocino is shown by underway measurements (Figure 16). The edges of the tongue of high salinity water were clearly delineated by two sharp fronts near 40.0°N and 40.5°N. Small-scale temperature minima coincided with each salinity front, but a regional change in temperature occurred only across the southern salinity front: water north of the high salinity tongue was nearly as cool as water within the tongue. As a result, density changes due to temperature and salinity reinforced each other across one front and partially compensated each other across the second. Both $\Delta D_{0/500}$ and the direct measurements show that the current jets were much broader than the surface density or salinity fronts, and the core of the onshore flowing jet was to the south of the surface front (Figure 16). There was broad enhancement of surface nutrients and chlorophyll in the high-density waters within and north of the high-salinity tongue, reflecting the relationship seen in Figure 9; nutrient levels were above 4 μM across most of the high salinity tongue, compared with averages of less than 1 μM to the south of the tongue. Local maxima in surface nutrients also were correlated with the local temperature minima, both at the salinity fronts and for two small features south of 40.0°N. These local peaks could be due to advection in the current jets, but they may also reflect local upwelling or mixing [*Washburn and Armi*, 1988; *Washburn et al.*, 1991; *Kadko et al.*, 1991]. It should be noted that the strongest cool, high nutrient peaks occur at the surface density fronts.

## 7. Seasonal Change in Vertical Structure

Seventy-three CTD stations between line I (150 km offshore) and line III (60 km offshore) were sampled during each of the March, May and June surveys; in addition, 38 CTD stations between lines I and III were sampled during February. These data were used to examine the structure of the fields with depth, and the seasonal variation of that structure. A mixed layer depth was determined for each of these

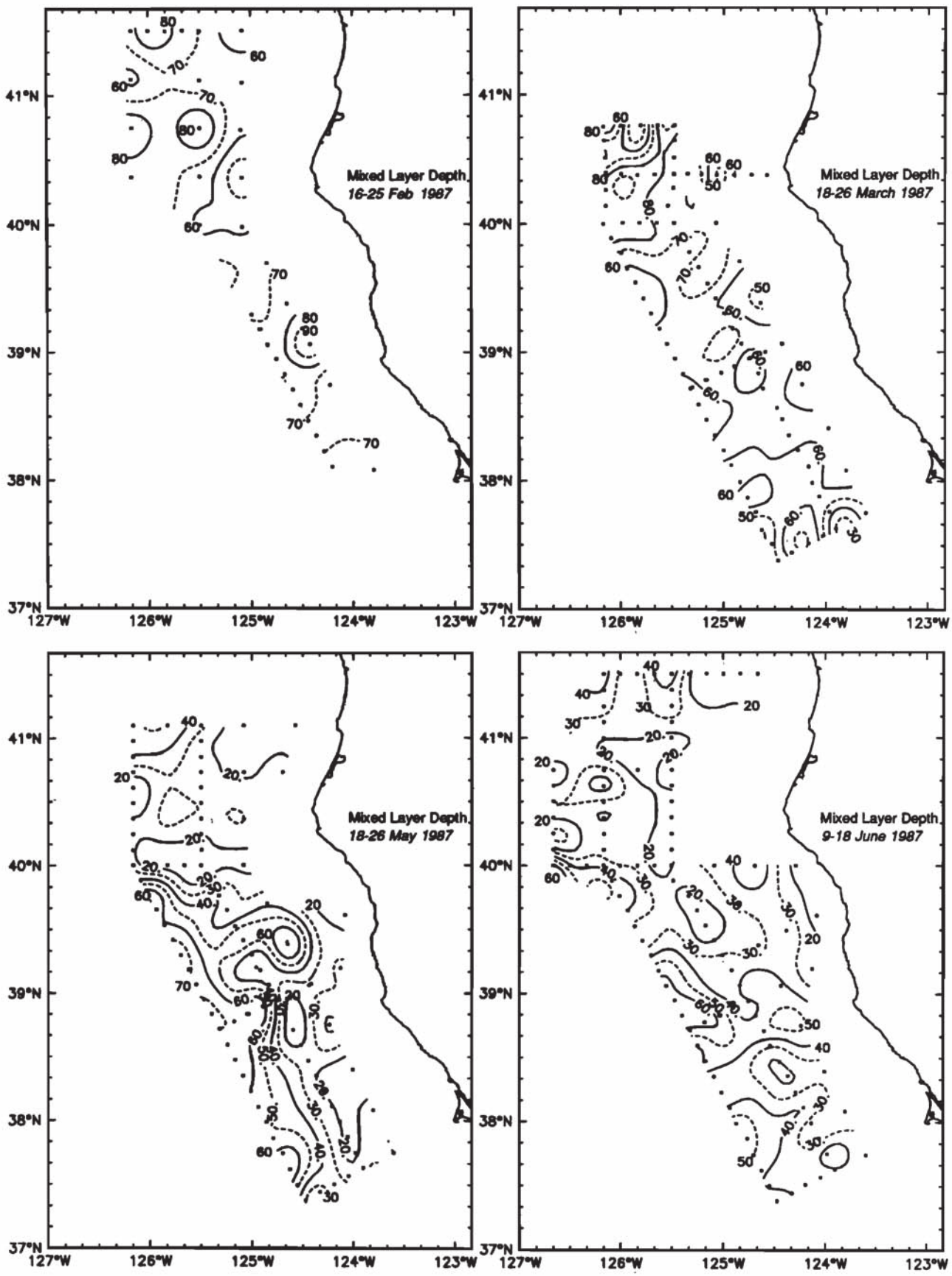


Fig. 17. Mixed layer depth (meters), defined [after *Davis et al.*, 1981] as the depth at which temperature changes by 0.1°C from the value at 10 m.

stations, based on a 0.1°C change from the temperature at 10 m [after *Davis et al.*, 1981]. Vertical profiles of the average and standard deviation in temperature, salinity, density anomaly and dynamic height were computed for each survey, as were the correlation between property distributions at different depths.

Mixed layers at most winter stations were deep, averaging 71 m in February and 64 m in March; only 2 of the 111 winter stations had mixed layers less than 40 m thick, and about 90% had mixed layers thicker than 50 m (Figure 17, Plate 1). Thus each average profile had a nearly uniform surface layer about 50 m thick (Figure 18). Standard deviations in temperature, salinity and density fields at a fixed depth were largest well below the surface; highest values were found near 85 m, where the average vertical gradients were strongest, suggesting that much of the horizontal variability was due to vertical displacements. Standard deviations in density were not much larger at the surface than at 250 m, and the well sampled March cruise had stronger temperature variation at 250 m than at the surface.

The spring profiles of averages and standard deviations in the coastal transition zone showed large differences from the winter profiles (Figure 18). Mixed layer depths averaged 38 m and 35 m in May and June, respectively. Shallow mixed layers were typically found inshore of the upwelling front; the correlation between mixed layer depth and $\Delta D_{0/500}$ (Figures 17 and 11; Plate 1) was 0.82 in May and 0.56 in June, both significant at the 95% confidence level. Average profiles were stratified all the way to the surface, reflecting the higher fraction of shallow mixed layer depths (nearly 25% less than 20 m). Below 50 m, the averages were cooler, saltier and more dense in spring than in winter, as would be expected in the presence of upwelling. The average temperature above 40 m was higher in spring than in winter, by as much as 0.6°C. A large winter-to-spring increase in variability at fixed depth was apparent over the upper 100 m in all fields, particularly the dynamic height. The highest variability in the temperature, salinity and density fields was still subsurface, but the peak was broader.

The change in season was accompanied by a change in the degree of correlation between fields at different depths (Figure 19). For the spring cruises, fields at different depths were well correlated over large vertical separations, and maps at one level strongly resembled those at another. This was especially true for the dynamic height field $\Delta D_{z/500}$, which is a vertical integral; maps of dynamic height at different depths were correlated at better than 0.8 over nearly all depths above 400 m. In winter, however, near-surface variability was not positively correlated with deep variability; in fact, both winter cruises showed density fluctuations near 80 m which were anticorrelated with density fluctuations below about 200 m (Figure 19). A subsurface eddy observed in March along line I contributes to this anticorrelation (Figure 20).

How much upwelling would be required to transform the winter fields into the spring ones? Figure 21 shows that, from March to May (or June), the average vertical displacement of isopycnals on each alongshore transect was surprisingly depth independent down to 450 m. Upwelling was clearly present on average along the lines 60 and 90 km offshore, but not along line I 150 km offshore. Maps of isopycnal displacements at several depths yield similar conclusions and show the close correspondence between the regions of large upwelling (Figure 22) and the region inshore of the meandering front and current jet (Figure 11).

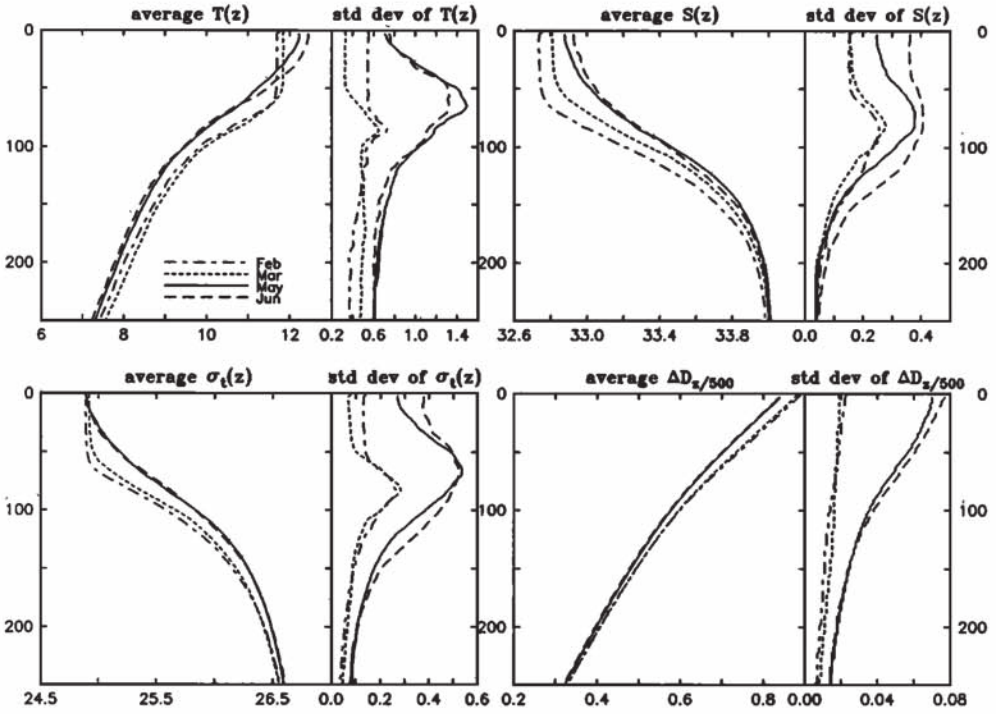


Fig. 18. Vertical profiles of horizontal averages and standard deviations of temperature, salinity, density anomaly $\sigma_t$ and dynamic height $\Delta D$ for the February (long dash-short dash), March (short dash), May (solid) and June (long dash) 1987 surveys. For March, May and June, the same 73 stations lying between 60 and 150 km offshore were averaged; in February, the 38 stations in this region were used.

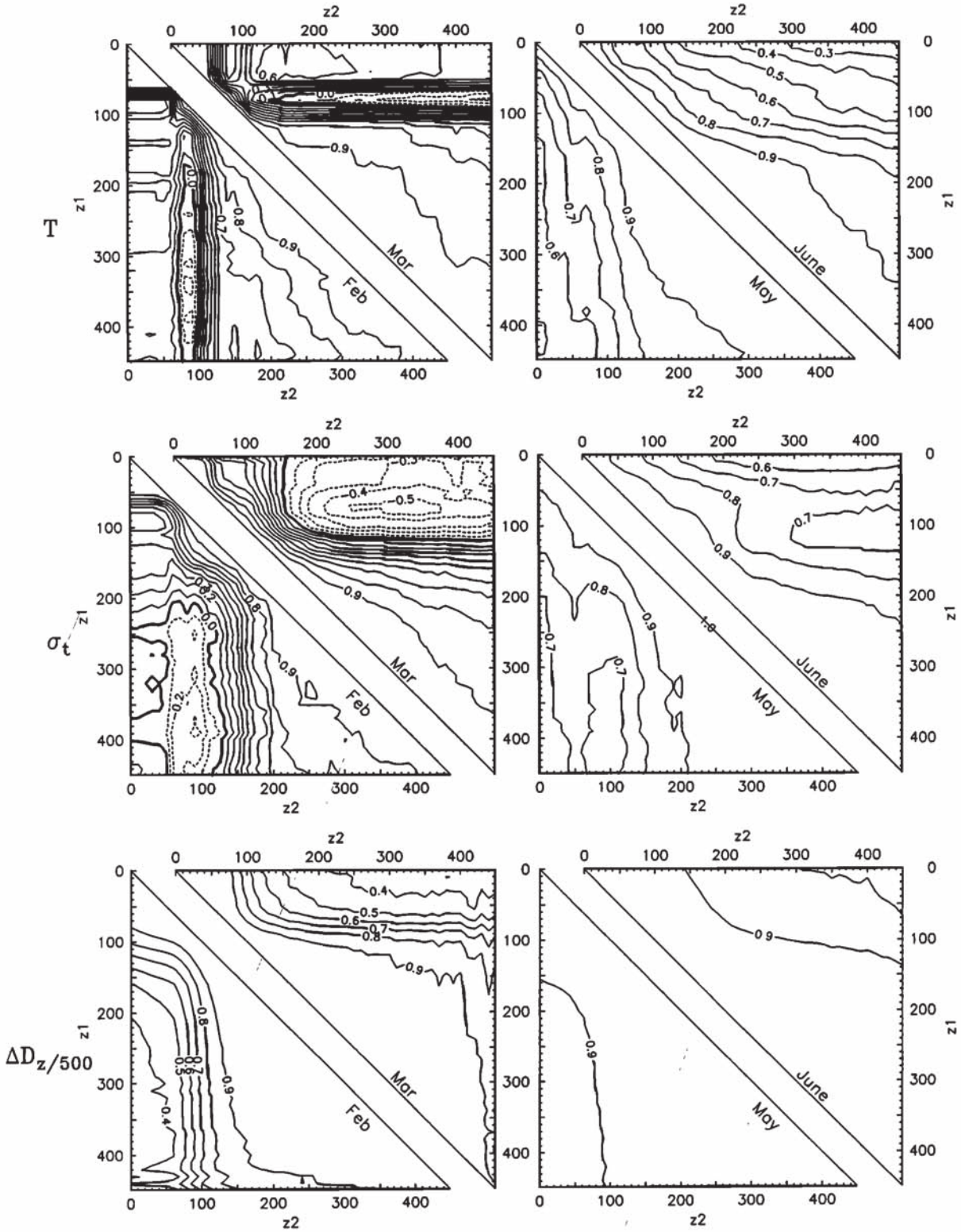


Fig. 19. Correlations between maps at different depths z1, z2, of temperature T, density anomaly $\sigma_t$ and dynamic height relative to 500 dbar $\Delta D_{z/500}$, for the February, March, May and June cruises. Data are from CTD casts along and between lines III (60 km offshore) and I (150 km offshore). Correlations above 0.3 (0.4) are expected to be significant at the 95% confidence level for T and $\sigma_t$ ($\Delta D_{z/500}$), based on the autocovariance functions of the fields (see main text).

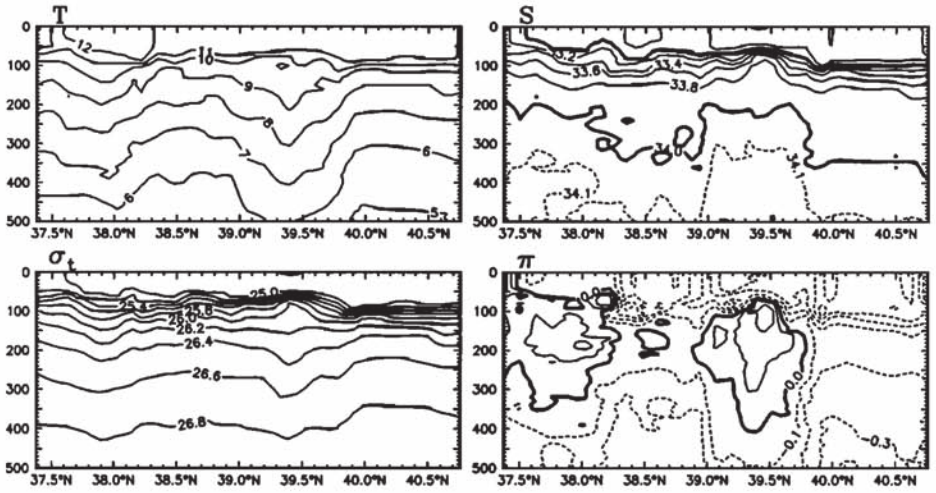


Fig. 20. Vertical sections of temperature, salinity, density anomaly $\sigma_t$ and spiciness $\pi$ along line I (150 km offshore) during March 1987 shows the presence of a subsurface eddy, with upwarping of isopycnals in and just below the pycnocline and downwarping of the isopycnals below. (Spiciness is a measure of thermohaline properties satisfying, in a least-squares sense, a generalized orthogonality condition with the density. It is calculated using the method of *Flament* [1986], and is high for warm, salty water. See also *Simpson and Lynn* [1990] and *Huyer et al.* [this issue]).

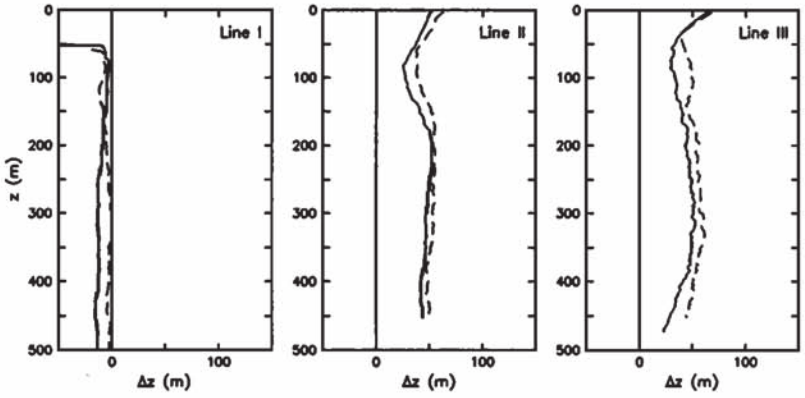


Fig. 21. Vertical displacement of the average isopycnal depths for May (solid) and June (long dash) relative to the average March values. Separate averages are presented for lines I, II and III, 60 km, 90 km and 150 km offshore respectively.

## 8. Summary and Discussion

The following picture emerges from these results: In late winter, surface waters of the coastal transition zone were characterized by deep mixed layers and weak horizontal variability; lateral gradients tended to be strong only below the mixed layer or near the coast. Sea level tended to be flat across the transition zone, with steric height $g^{-1}\Delta D_{0/500}$ averaging 0.90 m. By late spring, upwelling of dense water had yielded low sea levels near the coast (some steric heights $g^{-1}\Delta D_{0/500}$ lower than 0.8 m) and high sea levels were found offshore (some steric heights above 1.0 m). In the region between high and low sea level, a baroclinic current flowed, with the low-density, high-sea-level waters to the right of the current. The change from high to low sea level often occurred abruptly in an upwelled front; there, baroclinic current jets 30–50 km wide were found, with currents up to 1 m/s strong and transports of several sverdrups. These fronts meandered widely, but remained continuous over more than 100 km. Along-front current jets also meandered, and currents of comparable speed directed both toward and away from the coast were observed. Some meanders developed or decayed rapidly, on time scales of a few weeks; satellite imagery suggested that others persisted for many weeks. Surface waters enriched in nutrients and in chlorophyll were found inshore of the front. Seasonal upwelling, as measured by the vertical displacement of isopycnal surfaces from winter to spring, was found inshore of the meandering front; it extended deep into the water column, and appeared to be depth independent to a surprising degree. In May and June, a meander was observed straddling the Mendocino ridge, which rises from the seafloor to a depth of about 1500 m (see Figure 1); the presence of the ridge may be dynamically important in determining the position and intensity of meanders in the generally southward current.

What is the contribution of the baroclinic frontal jets observed in the CTZ region to the California Current? Lynn et al. [1982] present seasonal averages of hydrographic data

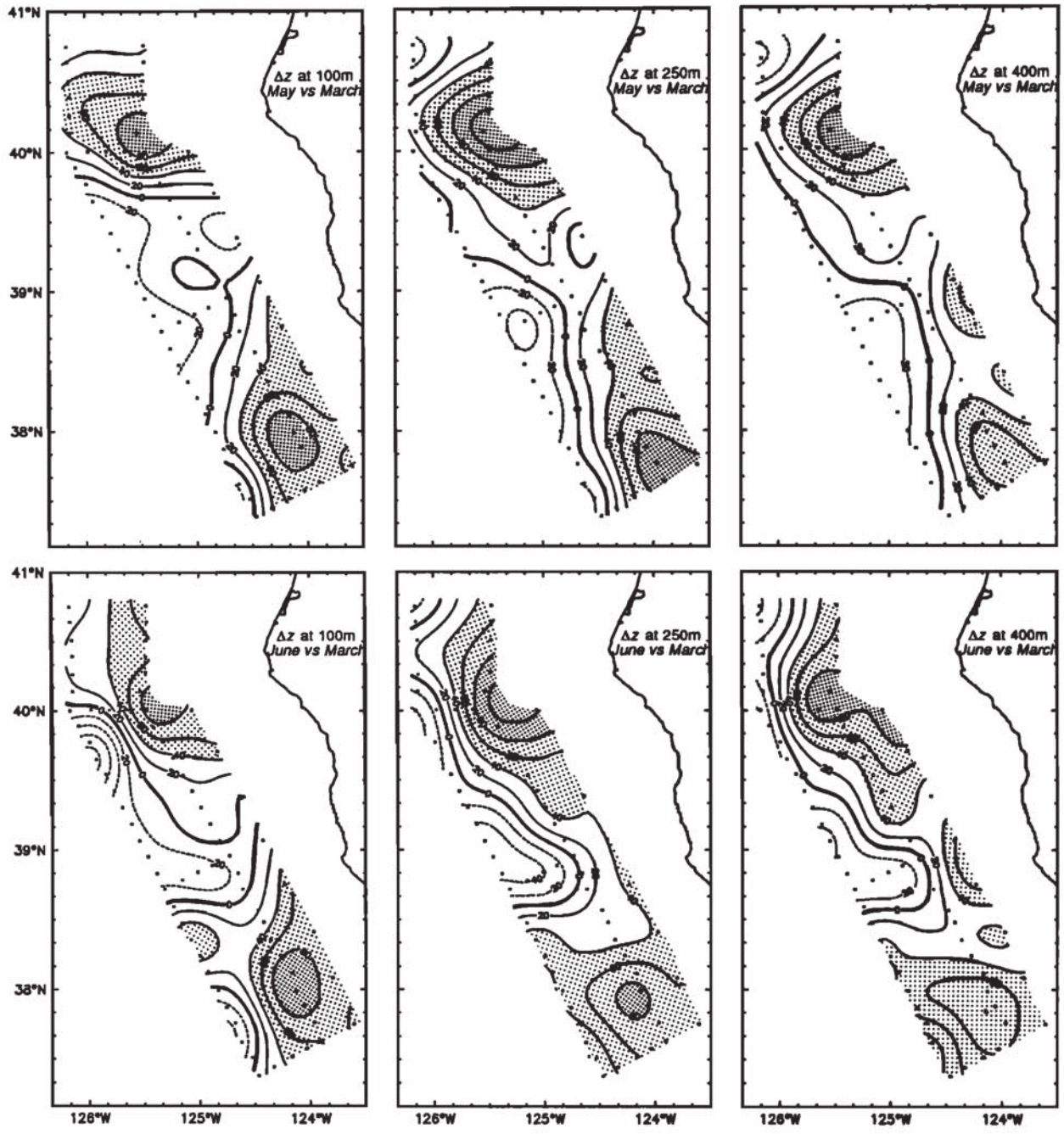


Fig. 22. Vertical displacement of the isopycnals at 100 m, 250 m and 400 m in May and June from their depth in March. Upwelling of more than 40 m (80 m) is shaded lightly (darkly).

collected across the California Current during the period 1950 to 1978 as part of the California Cooperative Oceanic Fisheries Investigations (CalCOFI) program. Their northernmost average is for CalCOFI line 60, which crosses the California Current offshore from Point Reyes (Figure 23). The baroclinic volume transport across this line is 2–4 Sv during the July season, depending on the choice of offshore limit (up to 800 km offshore). This is comparable to the transport in the frontal jets estimated from these surveys and from others [*Freitag and Halpern*, 1981; *Kosro and Huyer*, 1986], including the 1988 CTZ experiment [*Huyer et al.*, this issue]. Moreover, the surveys in May and June 1987 (Figure 11) showed steric height $g^{-1}\Delta D_{0/500}$ rising by 0.1–0.2 m across the upwelling front, from below 0.8 m inshore to above 0.9 m or 1.0 m offshore. Averages of historical data along repeated cross-shore transects at CalCOFI line 60 and at the 1981–1982 Coastal Ocean Dynamics Experiment (CODE) Central line [*Huyer*, 1984; *Huyer and Kosro*, 1987] also show values below 0.8 m near the coast, and both rise above 0.9 m with distance offshore (Figure 23). However, the average of steric height rises much more rapidly along the CODE Central line than it does off Point Reyes, about

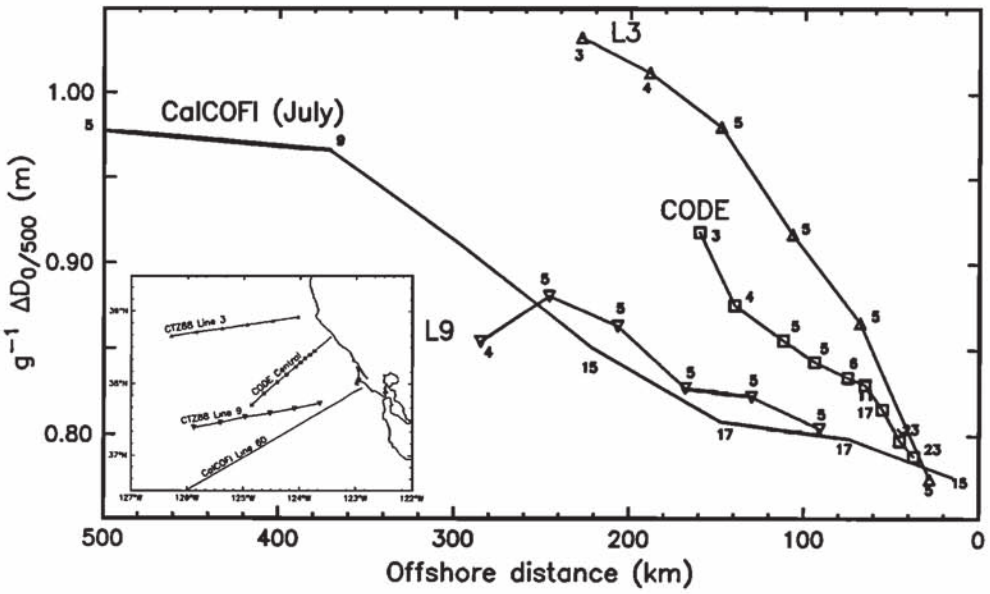


Fig. 23. Averages of steric height, $g^{-1}\ \Delta D_{0/500}$, as a function of distance offshore along four repeated transects: CalCOFI line 60 (data are from *Lynn et al.*, 1982, for the July "season", covering 1950–1978), CODE (data from 1981 and 1982, for the period April 23 to August 19), and for two of the repeated transects during the 1988 CTZ experiment (June 20 to Aug 4). The number of samples is plotted near the symbol for each station.

100 km to the south. Averages along repeated transects from the 1988 CTZ experiment support this result (Figure 23), indicating a narrower frontal zone north. These averages indicate a widening of the frontal zone south of Point Arena and suggest a connection between the frontal jets north of Point Reyes and a broader, more offshore California Current further south.

*Acknowledgements.* This work was supported by the Office of Naval Research, Coastal Sciences Section (Code 1122CS). We wish to thank John Borchardt and colleagues at EG&G for providing the wind and coastal sea level data, Melissa Ciandro and Bob Whritner at the Scripps Satellite Oceanography Facility for providing satellite imagery to the survey ships, and Rich Schramm, Jane Fleischbein, Henry Pittock and Robert Marsh for their contributions to the successful collection of the data presented here.

## REFERENCES

Abbott, M. R., and P. M. Zion, Satellite observations of phytoplankton variability during an upwelling event, *Cont. Shelf Res.*, *4*, 661-680, 1985.

Bernstein, R. L., L. Breaker, and R. Whritner, California Current eddy formation: Ship, air and satellite results, *Science*, *195*, 353-359, 1977.

Bretherton, F. P., R. E. Davis, and C. B. Fandry, A technique for objective analysis and design of oceanographic experiments applied to MODE-73, *Deep-Sea Res.*, *23*, 559-582, 1976.

Chereskin, T. K., E. Firing, and J. A. Gast, Identifying and screening filter skew and noise bias in Acoustic Doppler Current Profiler measurements, *J. Atmos. Oceanic Technol.*, *6*(6), 1040-1054, 1989.

Coastal Transition Zone Group, The Coastal Transition Zone Program, *Eos, Trans. AGU*, *69*(27), 698ff, 1988.

Davis, R. E., Drifter observations of coastal surface currents during CODE: The method and descriptive view, *J. Geophys. Res.*, *90*(C3), 4741-4755, 1985.

Davis, R. E., R. deSzoeke, D. Halpern, and P. Niiler, Variability in the upper ocean during MILE. Part I: The heat and momentum balances, *Deep-Sea Res.*, *28A*(12), 1427-1451, 1981.

Denman, K. L., and H. J. Freeland, Correlation scales, objective mapping and a statistical test of geostrophy over the continental shelf, *J. Mar. Res.*, *43*(3), 517-539, 1985.

Flament, P., Finestructure and subduction associated with upwelling filaments, Ph. D. dissertation, 142 pp, University of California, San Diego, 1986.

Flament, P., L. Armi, and L. Washburn, The evolving structure of an upwelling filament, *J. Geophys. Res.*, *90*(C6), 11,765-11,778, 1985.

Fofonoff, N. P., and R. C. Millard, Jr., Algorithms for computation of fundamental properties of sea water, Tech. Pap. in Mar. Sci., Vol. 44, 53 pp, UNESCO, Geneva, 1983.

Freitag, H. P., and D. Halpern, Hydrographic observations off northern California during May 1977, *J. Geophys. Res.*, *86*(C5), 4248-4252, 1981.

Halliwell, G. R. Jr., and J. S. Allen, The large-scale coastal wind field along the west coast of North America, 1981-1982, *J. Geophys. Res.*, *92*(C2), 1861-1884, 1987.

Hayward, T. L., and A. W. Mantyla, Physical, chemical and biological structure of a coastal eddy near Cape Mendocino, *J. Mar. Res.*, *48*(4), 825-850, 1990.

Holm-Hansen, O., C. J. Lorenzen, R. Holmes, and J. D. Strickland, Fluorometric determination of chlorophyll, *J. Cons. Perm. Int. Explor. Mer*, *30*, 3-15, 1965.

Hood, R. R., M. R. Abbott, and A. Huyer, Phytoplankton and photosynthetic light response in the coastal transition zone off northern California in June, 1987., *J. Geophys. Res.*, this issue.

Hood, R. R., M. R. Abbott, A. Huyer, and P. M. Kosro, Surface patterns in temperature, flow, phytoplankton biomass, and species composition in the coastal transition zone off northern California, *J. Geophys. Res.*, *95*(C10), 18,081-18,094, 1990.

Huyer, A., Hydrographic observations along the CODE Central Line off northern California, 1981, *J. Phys. Oceanogr.*, *14*(10), 1647-1658, 1984.

Huyer, A., and P. M. Kosro, Mesoscale surveys over the shelf and slope near Point Arena, California, *J. Geophys. Res.*, *92*(C2), 1655-1681, 1987.

Huyer, A., E. J. C. Sobey, and R. L. Smith, The spring transition in currents over the Oregon continental shelf, *J. Geophys. Res.*, *84*(C11), 6995-7011, 1979.

Huyer, A., P. M. Kosro, J. Fleischbein, S. R. Ramp, T. Stanton, L. Washburn, F. P. Chavez, T. J. Cowles, S. D. Pierce, and R. L. Smith, Currents and water masses of the coastal transition zone off northern California, June to August 1988, *J. Geophys. Res.*, this issue.

Ikeda, M., and W. J. Emery, Satellite observations and modeling of meanders in the California Current system off Oregon and northern California, *J. Phys. Oceanogr.*, *14*, 1434-1450, 1984.

Jessen, P. F., S. R. Ramp, and C. A. Clark, Hydrographic data from the pilot study of the Coastal Transition Zone (CTZ) program: 17-26 March 1987, report NPS-68-89-001, 210 pp, Dep. of Oceanogr., Nav. Postgrad. Sch., Monterey, Calif., Jan. 1989.

Johnson, K. S., and R. L. Petty, Determination of nitrate and nitrite in seawater by flow injection analysis, *Limnol. Oceanogr.*, *2*, 1260-1266, 1983.

Kadko, D. C., L. Washburn, and B. Jones, Evidence of subduction within cold filaments of the northern California coastal transition zone, *J. Geophys. Res.*, this issue.

Kosro, P. M., Shipboard acoustic current profiling during the Coastal Ocean Dynamics Experiment, Ph.D. dissertation, Univ. of Calif., San Diego, 1985.

Kosro, P. M., and A. Huyer, CTD and velocity surveys of seaward jets off northern California, July 1981 and 1982, *J. Geophys. Res.*, *91*(C6), 7680-7690, 1986.

Lentz, S. J., A description of the 1981 and 1982 spring transitions over the northern California shelf, *J. Geophys. Res.*, *92*(C2), 1545-1567, 1987.

Lynn, R. J., K. A. Bliss, and L. E. Eber, Vertical and horizontal distributions of seasonal mean temperature, salinity, sigma-t, dynamic height, oxygen and oxygen saturation in the California Current, 1950-1978, *CalCOFI Atlas 30*, 513 pp, Calif. Coop. Oceanic Fish. Invest., Univ. of Calif., La Jolla, 1982.

Magnell, B. A., N. A. Bray, C. D. Winant, C. L. Greengrove, J. Largier, J. F. Borchardt, R. L. Bernstein, and C. E. Dorman, Convergent shelf flow at Cape Mendocino, *Oceanography*, *3*(1), 4-11, 64, 1990.

Mooers, C. N. K., and A. R. Robinson, Turbulent jets and eddies in the California Current and inferred cross-shore transports, *Science*, *223*, 51-53, 1984.

Paduan, J. D., and P. P. Niiler, A Lagrangian description of motion in northern California coastal transition filaments, *J. Geophys. Res.*, *95*(C10), 18,095-18,109, 1990.

Pollard, R., and J. Read, A method for calibrating shipmounted acoustic Doppler profilers and the limitations of gyro compasses, *J. Atmos. Oc. Technol.*, *6*(6), 859-865, 1989.

Rienecker, M. M., and C. N. K. Mooers, A summary of the OPTOMA programs mesoscale ocean prediction studies in the California Current system, in *Mesoscale/Synoptic Coherent Structures in Geophysical Turbulence*, edited by J. C. J. Nihoul and B. M. Jamart, pp. 519-548, Elsevier Science, New York, 1989.

Rienecker, M. M., C. N. K. Mooers, D. E. Hagan, and A. R. Robinson, A cool anomaly off northern California: An investigation using IR imagery and in situ data, *J. Geophys. Res.*, *90*(C3), 4807-4818, 1985.

Rienecker, M. M., C. N. K. Mooers, and A. R. Robinson, Dynamical interpolation and forecast of the evolution of mesoscale features off northern California, *J. Phys. Oceanogr.*, *17*(8), 1189-1213, 1987.

Robinson, M. K., Atlas of North Pacific Ocean: monthly mean temperatures and mean salinities of the surface layer, *Ref. Publ. 2*, 173 pp, Nav. Oceanogr. Off., Washington, D.C., 1976.

Schramm, R. E., J. Fleischbein, A. Huyer, and P. M. Kosro, CTD Observations in the coastal transition zone off northern California 16-25 February 1987, Data Report 137, Ref. 87-24, 62 pp, Coll. of Oceanogr., Ore. State Univ., Sept. 1987.

Schramm, R. E., J. Fleischbein, R. Marsh, A. Huyer, P. M. Kosro, T. Cowles, and N. Dudek, CTD Observations in the coastal transition zone off northern California 18-27 May 1987, Data Report 141, Reference 88-3, 192 pp, College of Oceanography, Oregon State University, April 1988*a*.

Schramm, R. E., J. Fleischbein, A. Huyer, P. M. Kosro, T. Cowles, and N. Dudek, CTD Observations in the coastal transition zone off northern California 9-18 June 1987, Data Report 142, Ref. 88-4, 228 pp, Coll. of Oceanogr., Ore. State Univ., April 1988*b*.

Simpson, J. J., and R. J. Lynn, A mesoscale eddy dipole in the offshore California Current, *J. Geophys. Res.*, *95*(C8), 13,009-13,022, 1990.

Strub, P. T., J. S. Allen, A. Huyer, and R. L. Smith, Large-scale structure of the spring transition in the coastal ocean off western North America, *J. Geophys. Res.*, *92*(C2), 1527-1544, 1987.

Thomson, R. E., and J. E. Papadakis, Upwelling filaments and motion of a satellite-tracked drifter along the west coast of North America, *J. Geophys. Res.*, *92*(C6), 6445-6461, 1987.

Traganza, E. D., D. A. Nestor, and A. K. McDonald, Satellite observations of a nutrient upwelling off the coast of California, *J. Geophys. Res.*, *85*(C7), 4101-4106, 1980.

Venrick, E. L., and T. L. Hayward, Determining chlorophyll on the 1984 CALCOFI surveys, CALCOFI Rep. 25, 74-78 pp, Calif. Coop. Oceanic Fish. Invest., Univ. of Calif., La Jolla, 1984.

Walstad, L. J., J. S. Allen, P. M. Kosro, and A. Huyer, Dynamics of the coastal transition zone in 1987 through data assimilation studies, *J. Geophys. Res.*, this issue.

Washburn, L., and L. Armi, Observations of frontal instabilities on an upwelling filament, *J. Phys. Oceanogr.*, *18*(8), 1075-1092, 1988.

Washburn, L., D. C. Kadko, B. H. Jones, T. Hayward, P. M. Kosro, T. P. Stanton, S. Ramp, and T. Cowles, Water mass subduction and the transport of phytoplankton in a coastal upwelling system, *J. Geophys. Res.*, this issue.

Winant, C. D., R. C. Beardsley, and R. E. Davis, Moored wind, temperature, and current observations made during Coastal Ocean Dynamics Experiments 1 and 2 over the northern California continental shelf and upper slope, *J. Geophys. Res.*, *92*(C2), 1569-1604, 1987.

Wooster, W. S., and J. L. Reid, Jr., Eastern boundary currents, in *The Sea*, Vol. 2, edited by M. N. Hill, pp. 253-280, Interscience, New York, 1963.

Wyllie, J. G., Geostrophic flow of the California Current at the surface and at 200 meters, *CalCOFI Atlas 4*, 288 pp, Calif. Cooperative Oceanic Fish. Invest., Univ. of Calif., La Jolla, 1966.

---

M. R. Abbott, T. J. Cowles, A. Huyer, P. M. Kosro, L. F. Small, R. L. Smith and P. T. Strub, College of Oceanography, Oregon State University, Oceanography Administration Bldg. 104, Corvallis, OR 97331

R. T. Barber, Duke University Marine Laboratory, Pivers Islands, Beaufort, NC 28516.

F. P. Chavez, Monterey Bay Aquarium Research Institute, 160 Central Avenue, Pacific Grove, CA 93950

P. Jessen and S. R. Ramp, Department of Oceanography, Code 68, Naval Postgraduate School, Monterey, CA 93943

(Received October 23, 1990;
accepted April 1, 1991.)

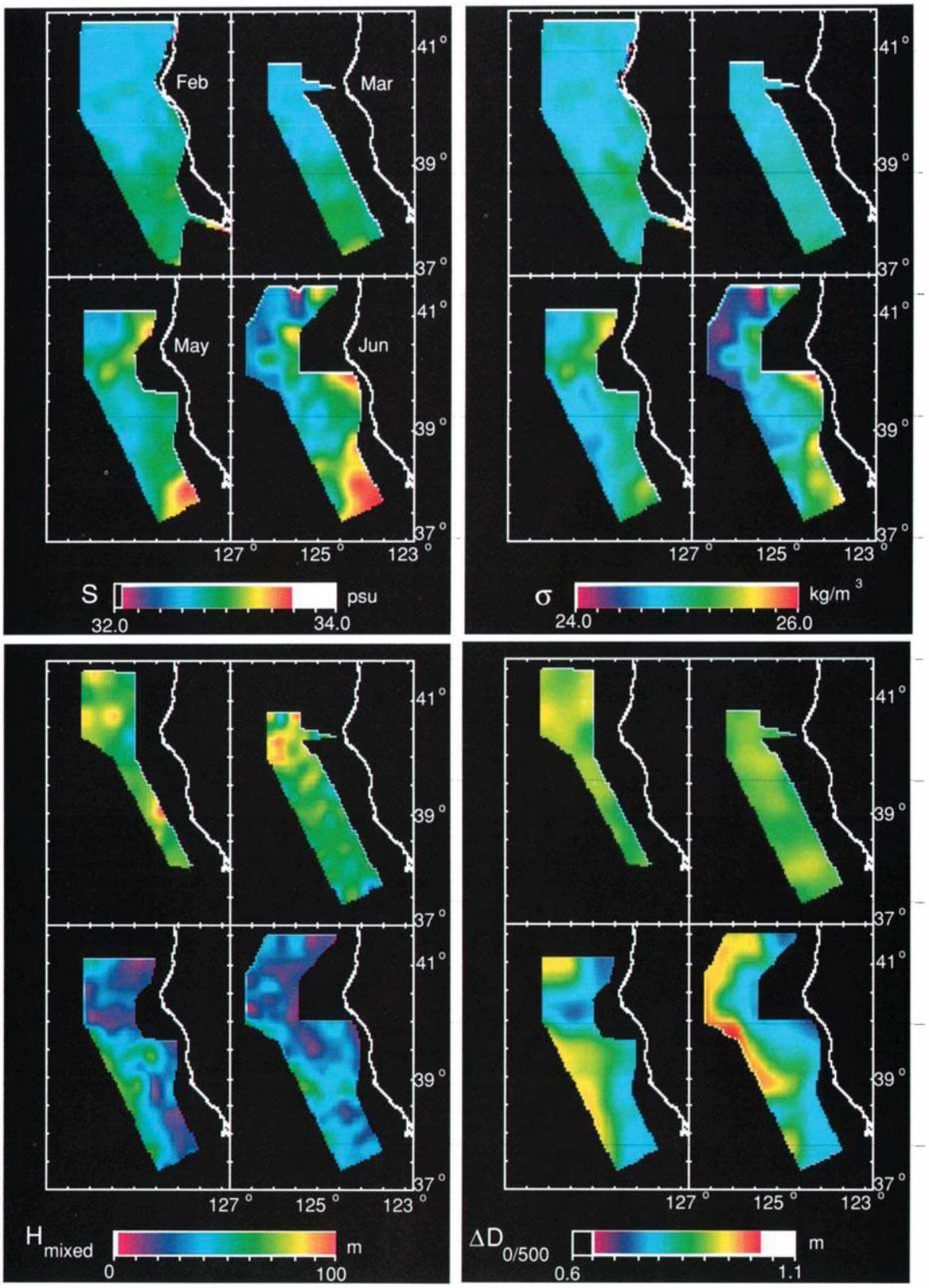


Plate 1. [*Kosro et al.*]. Objective maps of (top left) surface salinity, (top right) density anomaly, (bottom left) mixed layer depth and (bottom right) dynamic height relative to 500 dbar for each of four cruises (February, March, May and June, 1987). See Figures 5, 6, 11 and 17 for black and white versions.